NASA Technical Memorandum 84475

Automated Optimum Design of Wing Structures

Deterministic and Probabilistic Approaches

S. S. Rao

AUGUST 1982

NASA

NASA Technical Memorandum 84475

Automated Optimum Design of Wing Structures

Deterministic and Probabilistic Approaches

S. S. Rao
Langley Research Center
Hampton, Virginia

National Aeronautics
and Space Administration

Scientific and Technical Information Office

1982

CONTENTS

SUMMARY

A procedure is described for the automated optimum design of airplane wing structures subjected to multiple behavior constraints. The structural mass of the wing is considered the objective function. The maximum stress, wing tip deflection, root angle of attack, and flutter velocity during the pull-up maneuver (static load), the natural frequencies of the wing structure, and the stresses induced in the wing structure due to landing and gust loads are suitably constrained. Both deterministic and probabilistic approaches are used for finding the stresses induced in the airplane wing structure due to landing and gust loads.

The procedure is illustrated with two examples. The first is a wing represented by a uniform beam with a cross section in the form of a hollow symmetric double wedge. The airfoil thickness and chord length are the design variables, and a graphical procedure is used to find the optimum solutions. The second example is a supersonic wing represented by finite elements. The thicknesses of the skin and the web and the cross-sectional areas of the flanges are the design variables, and nonlinear programming techniques are used to find the optimum solution.

For the examples considered, the optimum value of the objective function is higher when the landing and gust stresses are treated as random variables than when they are considered deterministic quantities.

INTRODUCTION

Considerable progress has been made in airplane structural optimization over the last two decades. Several investigators have considered both strength and aeroelastic requirements in airplane optimum structural design problems. In reference 1, a double-wedge airfoil is idealized as a bar, and a steepest descent method is used to minimize the total energy required to drive the airfoil through a specified flight condition. The behavior constraints considered in the optimization are the root angle of attack, the elastic deflection at the leading edge of the wing tip, the principal stress in the skin at the root of the wing, and the Mach number of bending-torsion flutter. The automated preliminary design of wing structures was considered in references 2 and 3 by idealizing the wing as a plate. In reference 2, the wing is idealized as an isotropic sandwich plate with a variable thickness cover, and an interior penalty function method is used to minimize the weight of the cover by varying its thickness distribution. The method of feasible directions is used in reference 3 to determine a simplified configuration of the wing structure, wing depth distribution, and cover panel thickness distribution by minimizing a linear combination of the aerodynamic drag and the weight of the wing.

Optimization techniques were applied in references 4 to 6 to minimize the mass of wing structures represented by finite elements. Reference 4 used the interior penalty function method of optimization with strength, frequency, and flutter as constraints. Reference 5 describes a computer program for the design of minimum mass wing structures under flutter, strength, and minimum gage constraints. In reference 6, a system of integrated computer programs is used for sizing structural member cross sections to satisfy strength and flutter design requirements for several variants of an arrow wing supersonic cruise vehicle. The resulting structural weights

are used to determine the structural efficiency of the planform geometry, structural layout, type of construction, and type of material including composites. Several authors (refs. 7 and 8) have also considered the optimum design of structures with the material properties and loads treated as probabilistic quantities. However, probabilistic approaches to the design of airplane structures appear to be applied rarely.

The present work presents a procedure for the automated optimum design of airplane wing structures which limits the stresses developed due to landing and gust loads while considering static strength and flutter constraints. The dynamic loads resulting from the landing impact of airplanes contribute significantly to structural fatigue. In addition, the associated induced vibrations contribute to crew and passenger discomfort. Ground-induced dynamic loads and vibrations and the resulting problems will be magnified for supersonic cruise airplanes because of the increased structural flexibility of the slender body, thin-wing configuration and the higher take-off and landing speeds. Similarly, the dynamic stresses developed in an airplane structure in flight due to atmospheric gusts are very important and often control the design of wings of large airplanes. Since the contact conditions during landing (such as sink speed, horizontal speed at the instant before contact, and rolling velocity) and the vertical velocity due to gusts are random in nature, exact values of the stresses induced in the airplane wing structure due to landing and gusts cannot be specified. Hence, the design optimization problem is solved twice, first by using a deterministic approach and then by using a probabilistic approach for the computation of the landing and gust stresses. The material properties are assumed to be deterministic in both the approaches.

Two numerical examples are presented for demonstrating the feasibility of the method presented. First, the thickness and chord length of a uniform hollow double-wedge airfoil were determined with the help of graphical optimization techniques. In the second example, the thicknesses of cover skin and webs and the cross-sectional areas of flanges of a multiweb supersonic wing structure were found by using finite-element idealization and nonlinear programming techniques. The procedure described in this work is expected to be useful during preliminary design of an airplane.

SYMBOLS

a lift-curve slope

c chord

c_o reference chord

D total drag

D_f friction drag

D_p pressure drag

f objective function

F force transmitted by the landing gear

F_g force between the tire and the ground

g	acceleration due to gravity
g_j	jth constraint function
H	amplitude of the frequency response function
K_L	lift factor
ℓ	semispan of double-wedge airfoil (example 1)
L	scale of turbulence
$L(x,y)$	lift distribution
m	total number of constraints
m_u	unsprung mass below shock strut
$m(x,y)$	mass distribution
M	flight Mach number
M_i	generalized mass in ith mode
n	number of design variables
N	number of segments of the airfoil (example 1)
p	number of natural frequencies constrained
p_∞	atmospheric pressure
Q_i	generalized force in ith mode
r	number of natural modes considered in the modal analysis
S	standard deviation
t	airfoil thickness
T_∞	atmospheric temperature
u	vertical velocity of the gust
U	flight velocity
V_F	flutter speed
V_g	forward velocity of flight at the time of gust encounter
V_ℓ	horizontal velocity at the instant before contact (during landing)
V_v	sinking velocity of the airplane
w_u	deflection of the unsprung mass

$w(x,y,\tau)$ deflection of the middle surface of the wing

$W^{(i)}(x,y)$ ith natural mode shape

x,y coordinates in the middle plane of the wing

x_i ith design variable

x_ℓ, y_ℓ coordinates of the landing gear attachment point

$\vec{X}$ design vector

y_i ith random variable

z vertical coordinate of wing

α,β constants in tire force-deflection relation

α_i variation of angle of attack of ith segment of the airfoil (example 1)

α_o root angle of attack

γ ratio of specific heats

δ wing tip deflection

$\xi_i(\tau)$ ith generalized coordinate

ρ density of air

ρ_m density of the material of the wing

ρ_s solidity ratio

σ_g maximum gust stress

σ_ℓ maximum landing stress

σ_s maximum steady-state stress

τ time

τ_d time at which the shock strut starts deflecting after initial contact of the tire with the ground

τ_f duration of flight

$\phi(\tau)$ random disturbance

$1 - \phi(\tau)$ Wagner function

$\Phi(\omega)$ power spectral density

$\psi(\tau)$ Küssner function; also random response of the system

$\phi(y_1, y_2, \ldots, y_q)$ function of random variables

ω_i ith natural frequency

Superscripts:

* value at the optimum point

ℓ lower bound

u upper bound

Subscripts:

b bending

t torsional

A bar over a symbol denotes mean value. A dot over a symbol denotes partial differential with respect to time.

FORMULATION OF OPTIMIZATION PROBLEM AND SOLUTION PROCEDURE

Loads Considered

The following load conditions are considered in formulating the problem:

1. The condition that exists during a longitudinal pull-up maneuver is considered the static load condition. The root angle of attack and the deformed shape of the wing, which provide the specified gross lift, are determined. Then the stress distribution and, hence, the maximum principal stress at the wing root corresponding to the static displacement state are then computed.

2. The landing load condition consists of the dynamic loads developed in the flexible wing structure during landing. Representative values of vertical (sink) velocity, forward velocity, and landing gear characteristics of the airplane are assumed. The interaction between the landing gear and the deformation of the airplane structure is considered in finding the landing load history after initial touchdown. From this computed load history, the stress variation and, hence, the maximum principal stress at the wing root during landing are determined. Since landing conditions such as sink velocity, forward velocity, and rolling speed are uncertain, they are treated as random variables in the probabilistic approach.

3. The gust load condition consists of the loads developed in the flexible airplane flying through a specified vertical gust. The vertical gust velocity distribution is assumed to be cosine type with known maximum value. The time variation of the gust loads and, hence, the stress distribution in the aircraft wing is computed by considering the gust magnitude to be constant in the spanwise direction. The random and continuous nature of the atmospheric turbulence is accounted for by assuming the gust velocity to be a stationary random process in the probabilistic approach.

Problem Formulation

A general design optimization problem involves determining the design variable vector

$$\vec{X}^* = \begin{Bmatrix} x_1^* \\ x_2^* \\ \vdots \\ x_n^* \end{Bmatrix} \tag{1}$$

which minimizes the objective function $f(\vec{X})$ subject to the constraints

$$g_j(\vec{X}) \leq 0 \qquad (j = 1, 2, \ldots, m) \tag{2}$$

In this work, the objective function is the structural mass of the wing. In the first example, the total energy required to drive the airfoil through a specified flight condition is an alternative objective function. The following constraints are considered in the formulation of the problem.

Natural frequency constraints.- The first p natural frequencies of the structure ω_i are to lie between specified lower and upper bounds. Thus,

$$\left.\begin{aligned} g_i(\vec{X}) &= \left(\omega_i^{\ell}/\omega_i\right) - 1 \leq 0 \qquad (i = 1, 2, \ldots, p) \\ g_{p+i}(\vec{X}) &= \left(\omega_i/\omega_i^{u}\right) - 1 \leq 0 \qquad (i = 1, 2, \ldots, p) \end{aligned}\right\} \tag{3}$$

Flutter constraint.- The flutter speed, V_F at a specified altitude is to be greater than a prescribed value V_F^{ℓ}. Thus,

$$g_{2p+1}(\vec{X}) = \left(V_F^{\ell}/V_F\right) - 1 \leq 0 \tag{4}$$

Deflection constraint.- The deflection of the wing tip δ under a specified steady-state design condition is to be less than the maximum permissible value δ^u. Thus,

$$g_{2p+2}(\vec{X}) = \left(\delta/\delta^{u}\right) - 1 \leq 0 \tag{5}$$

Angle of attack constraint.- The root angle of attack of the wing α_o under a given steady-state design condition is to be less than a specified maximum value α_o^u. Thus,

$$g_{2p+3}(\vec{X}) = \left(\alpha_o/\alpha_o^{u}\right) - 1 \leq 0 \tag{6}$$

Steady-state stress constraint.- The maximum principal stress induced at the root of the wing σ_s during a prescribed steady-state design condition is to be less than the maximum permissible value σ_s^u. Thus,

$$g_{2p+4}(\vec{X}) = \left(\sigma_s/\sigma_s^u\right) - 1 \leq 0 \tag{7}$$

Dynamic stress constraints.- The maximum principal stress induced at the root of the wing during landing σ_ℓ is to be less than the specified maximum value σ_ℓ^u. Thus,

$$g_{2p+5}(\vec{X}) = \left(\sigma_\ell/\sigma_\ell^u\right) - 1 \leq 0 \tag{8}$$

The maximum principal stress at the root of the wing due to specified gust conditions σ_g is to be less than the permissible value σ_g^u. Thus,

$$g_{2p+6}(\vec{X}) = \left(\sigma_g/\sigma_g^u\right) - 1 \leq 0 \tag{9}$$

Equations (7) to (9) assume that the maximum principal stress theory of failure is used instead of the more commonly used Von Mises theory. Further, the maximum stress may be induced at a point other than the root of the wing. Hence, for a more accurate formulation of the stress constraints, the maximum stress obtained by considering all the points of the structure is to be used in place of the maximum principal stress induced at the root of the wing in equations (7) to (9).

Side constraints.- The design variables x_i are to take values between specified lower and upper limits. Thus,

$$g_{2p+6+i}(\vec{X}) = \left(x_i^\ell/x_i\right) - 1 \leq 0 \qquad (i = 1, 2, \ldots, n) \tag{10}$$

$$g_{2p+n+6+i}(\vec{X}) = \left(x_i/x_i^u\right) - 1 \leq 0 \qquad (i = 1, 2, \ldots, n) \tag{11}$$

Solution Procedure

The nonlinear optimization problem stated in equations (1) and (2) is solved by the following techniques.

1. For the first example, which involves only two design variables (n = 2), a graphical optimization procedure is used (ref. 9).

2. For the second example, which involves more than two design variables, the Zoutendijk's method of feasible directions, coded in a program called CONMIN (ref. 10), is used for finding the optimum solution.

ANALYSIS

As stated earlier, the optimum design problem is solved by using a deterministic as well as a probabilistic approach for the computation of the stresses developed in the wing structure due to landing and gust loads. The uncertain parameters influencing the landing and gust loads are assumed to be random variables with known mean values and standard deviations. In the deterministic approach, the mean values plus three corresponding standard deviations are used as the representative values for these parameters. These representative values will not be exceeded 99.97 percent of the time if the uncertain parameters follow the normal distribution.

In the probabilistic approach, the mean values and standard deviations of the response quantities (stresses) are computed by using the mean values and standard deviations of the uncertain parameters, and the landing and gust stress constraints become

$$\frac{\sigma_\ell}{\sigma_\ell^u} - 1 = \frac{\bar{\sigma}_\ell + 3S_{\sigma_\ell}}{\sigma_\ell^u} - 1 \leqslant 0 \tag{12}$$

and

$$\frac{\sigma_g}{\sigma_g^u} - 1 = \frac{\bar{\sigma}_g + 3S_{\sigma_g}}{\sigma_g^u} - 1 \leqslant 0 \tag{13}$$

where the bar over a symbol denotes the mean and S the standard deviation of the landing stress (σ_ℓ) and gust stress (σ_g). If σ_ℓ and σ_g follow the normal distribution, the constraints of equations (12) and (13) correspond to a confidence level of 99.97 percent.

A brief outline of the landing and gust stress analyses according to deterministic and probabilistic approaches is given below.

Deterministic Approach

Landing analysis.- The stresses developed in the wing during landing are computed by considering the interaction between the landing gear and the flexible airplane structure. The landing gear is assumed to have nonlinear characteristics typical of conventional gears, namely, velocity squared damping, polytropic air-compression springing, and exponential tire force-deflection characteristics. The derivation of the coupled nonlinear differential equations of motion that arise in the landing analysis and their numerical solution follow closely the procedure outlined in reference 11.

According to the procedure described in reference 11, the displacement of the middle surface of the structure is expressed in terms of its natural modes of vibration as

$$w(x,y,\tau) = \sum_{i=0}^{r} W^{(i)}(x,y)\ \xi_i(\tau) \tag{14}$$

where $W^{(i)}(x,y)$ is the ith natural mode shape ($i = 0$ indicates the rigid body translation mode with $W^{(0)}(x,y) = 1$) and $\xi_i(\tau)$ is the ith generalized coordinate. Equation (14) shows that the first r natural modes are used in approximating the displacement of the airplane wing structure. If $w(x_\ell,y_\ell,\tau)$ denotes the transverse displacement of the landing gear attachment point (x_ℓ,y_ℓ), then from equation (14), one can write

$$w_\ell(\tau) = w(x_\ell,y_\ell,\tau) = \sum_{i=0}^{r} W_\ell^{(i)}\ \xi_i(\tau) \tag{15}$$

where $W_\ell^{(i)}$ denotes the value of $W^{(i)}(x,y)$ at (x_ℓ,y_ℓ). The equations of motion of the structure with the landing gear arrangement shown in figure 1 can be derived in terms of generalized coordinates as follows (ref. 11):

$$M_i\ \ddot{\xi}_i(\tau) + M_i\omega_i^2\ \xi_i(\tau) = Q_i \qquad (i = 0,\ 1,\ 2,\ \ldots,\ r) \tag{16}$$

and

$$Q_i = -FW_\ell^{(i)} - \iint_{\substack{\text{Wing}\\ \text{area}}} \left[L(x,y) - g\ m(x,y)\right] W^{(i)}(x,y)\ dx\ dy \qquad (i = 0,\ 1,\ 2,\ \ldots,\ r) \tag{17}$$

where M_i is the generalized mass of the structure in the ith mode (M_0 is the total mass of the structure), ω_i is the natural frequency of vibration in the ith mode ($\omega_0 = 0$), Q_i is the generalized force in the ith mode, F is the force transmitted by the landing gear, $L(x,y)$ is the lift distribution on the wing, $m(x,y)$ is the mass distribution of the wing, and g is the acceleration due to gravity.

Since the oleo-pneumatic shock struts are preloaded with air, they do not deflect until some time τ_d after the initial contact of the tire with the ground. During the time $0 \leqslant \tau \leqslant \tau_d$, which can be called the first stage of impact, the shock strut is effectively rigid; thus the deflections of the unsprung mass and the landing gear attachment point can be taken to be same ($w_\ell(\tau) = w_u(\tau)$) for small values of θ, the inclination of the shock strut. The motion of the complete system of landing gear and airplane is governed only by the force between the tire and the ground (F_g). During the subsequent time $\tau > \tau_d$, which can be called the second stage of impact, the shock strut starts to deflect; the motions of the landing gear attachment point and the unsprung mass are different ($w_\ell(\tau) \neq w_u(\tau)$). Hence, the equation of motion of the unsprung mass must be considered separately. Thus, the governing equations are different in the two stages.

For $0 \leq \tau \leq \tau_d$, the governing equations are given by equation (16) with

$$F = F_g + m_u \ddot{w}_u - m_u g \tag{18}$$

and F_g can be expressed by an exponential variation of tire force with deflection:

$$F_g = \alpha(w_u)^\beta \tag{19}$$

where α and β are constants and $w_u(\tau) = w_\ell(\tau)$.

For $\tau > \tau_d$, both $w_u(\tau)$ and $w_\ell(\tau)$ are treated as unknowns in equation (16). Since F is a nonlinear function of w_u, which can be expressed in terms of ξ_i using equation (14), equation (16) represents a set of r nonlinear differential equations.

In this work, the equations of motion are solved by using only the first flexural mode in addition to the rigid body mode (i.e., $r = 1$). The initial conditions for the first phase of impact, $0 \leq \tau \leq \tau_d$, are assumed to be

$$\left.\begin{aligned} \xi_0(\tau=0) &= 0 \\ \dot{\xi}_0(\tau=0) &= V_v \end{aligned}\right\} \tag{20}$$

where V_v is the vertical (sink) velocity of the airplane at the time of initial contact with the ground. The total lift of the wing (L_{total}) is assumed to be

$$L_{total} = \iint_{\substack{\text{Wing} \\ \text{area}}} L(x,y)\, dx\, dy = W_{total} K_L \tag{21}$$

where W_{total} is half the gross weight of the airplane and K_L is the lift factor. The initial conditions for the second phase of impact, $\tau > \tau_d$, are the terminal conditions of the first phase. A step-by-step numerical solution procedure (ref. 11) is used to find the values of the generalized coordinates $\xi_0(\tau)$ and $\xi_1(\tau)$ at $\tau = 0, \Delta\tau, 2\,\Delta\tau, \ldots$, where $\Delta\tau$ is a small time increment.

Once the values of $\xi_0(\tau)$ and $\xi_1(\tau)$ are known, the transverse displacement of the middle surface of the wing structure can be obtained as

$$w(x,y,\tau) = \xi_0(\tau) + w^{(1)}(x,y)\, \xi_1(\tau) \qquad (\tau = 0, \Delta\tau, 2\,\Delta\tau, \ldots) \tag{22}$$

With the known deflection $w(x,y,\tau)$, the stresses induced in the wing structure at various instants of time can be found from the basic relations of structural mechanics. The maximum principal stress developed near the root of the wing (σ_ℓ), during the total time interval considered for the analysis, can then be found without much difficulty.

Gust analysis.- To find the stresses developed in the wing due to a gust, the equations of motion of the aircraft are formulated with the vertical motion and wing bending modes as generalized coordinates. The gust is considered discrete and uniform along the span of the wing.

The transverse displacement of the middle surface of the wing can again be expressed by equation (14), and the equations of motion in terms of the generalized coordinates $\xi_i(\tau)$, by equation (16). The generalized force in the ith mode Q_i is given by

$$Q_i = \iint_{\substack{\text{Wing}\\ \text{area}}} F(x,y,\tau)\, W^{(i)}(x,y)\, dx\, dy \tag{23}$$

where $F(x,y,\tau)$ denotes the applied force distribution on the wing. By neglecting the effect of chordwise bending of the wing and using a strip type of analysis, equation (23) can be expressed as (refs. 12 and 13)

$$Q_i = \int_{\substack{\text{Wing}\\ \text{span}}} F(y,\tau)\, W^{(i)}(y)\, dy \tag{24}$$

with

$$\begin{aligned} F(y,\tau) = &- \frac{a\rho c_o V_g}{2} \int_0^\tau \ddot{w}(y,\tau)\left[1 - \phi(\tau-\tau')\right] d\tau' \\ &+ \frac{a\rho c_o V_g}{2} \int_0^\tau \dot{u}(\tau)\, \phi(\tau-\tau')\, d\tau' \end{aligned} \tag{25}$$

where the time τ is zero at the start of the gust penetration, a is the lift-curve slope, ρ is the density of air, c_o is the reference chord, V_g is the forward velocity of flight, $\ddot{u}$ is the vertical velocity of the gust, $[1 - \phi(\tau)]$ is the Wagner function, and $\phi(\tau)$ is the Kussner function. The lift-curve slope a may be chosen to correct approximately for aspect ratio and compressibility effects.

With equations (23) to (25), equation (16) for $i = 0$ and 1 can be written, after some mathematical manipulation, as a set of two simultaneous integral-differential equations (similar to eqs. (16) and (19) of ref. 12). These equations of motion are solved for the generalized coordinates $\xi_0(\tau)$ and $\xi_1(\tau)$ at the discrete time stations $\tau = 0, \Delta\tau, 2\,\Delta\tau, \ldots$, by using the numerical procedure outlined in reference 12 and by assuming that the airplane is in level flight before encountering the gust. The variation of the vertical gust velocity with time is assumed to be a cosine with known amplitude. Once the generalized coordinates $\xi_0(\tau)$ and $\xi_1(\tau)$ are known, the transverse displacement $w(x,y,\tau)$, the stresses induced, and hence σ_g, the maximum gust stress induced at the root of the wing, can be computed from the standard relations of structural mechanics.

Probabilistic Approach

Landing analysis.- Results of measurements of contact (touchdown) conditions of several transport airplanes made during routine daylight operations in clear air are given in reference 14. It was found that the contact conditions such as sink speed, horizontal speed at the instant before contact, and rolling velocity, although treated as constants in the deterministic analysis, are really random in nature. Since a function of several random variables is also random, the maximum landing stress should be treated as a random variable. Let ψ denote a general function of the independent random variables $(y_1, y_2, \ldots, y_q)$ whose mean values $(\bar{y}_1, \bar{y}_2, \ldots, \bar{y}_q)$ and standard deviations $\left(S_{y_1}, S_{y_2}, \ldots, S_{y_q}\right)$ are known; then the approximate values of the mean and standard deviation of ψ can be determined as (ref. 15)

$$\bar{\psi} \approx \psi(\bar{y}_1, \bar{y}_2, \ldots, \bar{y}_q) \tag{26}$$

and

$$S_\psi \approx \left[\sum_{i=1}^{q} \left(\frac{\partial \psi}{\partial y_i}\bigg|_{\bar{y}_1, \bar{y}_2, \ldots, \bar{y}_q}\right)^2 S_{y_i}^2\right]^{1/2} \tag{27}$$

In this work, the sink speed (V_v) and the horizontal speed at the instant before contact (V_ℓ) are taken as normally distributed and independent random parameters, so that

$$\bar{\sigma}_\ell \approx \sigma_\ell(\bar{V}_v, \bar{V}_\ell) \tag{28}$$

and

$$S_{\sigma_\ell} \approx \left[\left(\frac{\partial \sigma_\ell}{\partial V_v}\bigg|_{\bar{V}_v, \bar{V}_\ell}\right)^2 S_{V_v}^2 + \left(\frac{\partial \sigma_\ell}{\partial V_\ell}\bigg|_{\bar{V}_v, \bar{V}_\ell}\right)^2 S_{V_\ell}^2\right]^{1/2} \tag{29}$$

The partial derivatives of the maximum landing stress appearing in equation (29) are evaluated by using a finite-difference scheme:

$$\frac{\partial \sigma_\ell}{\partial V_v}\bigg|_{\bar{V}_v, \bar{V}_\ell} \approx \frac{\sigma_\ell(\bar{V}_v + \Delta V_v, \bar{V}_\ell) - \sigma_\ell(\bar{V}_v, \bar{V}_\ell)}{\Delta V_v} \tag{30}$$

and

$$\frac{\partial \sigma_\ell}{\partial V_\ell}\bigg|_{\bar{V}_v, \bar{V}_\ell} \approx \frac{\sigma_\ell(\bar{V}_v, \bar{V}_\ell + \Delta V_\ell) - \sigma_\ell(\bar{V}_v, \bar{V}_\ell)}{\Delta V_\ell} \tag{31}$$

where ΔV_v and ΔV_ℓ are small increments in the values of $\bar{V}_v$ and $\bar{V}_\ell$, and $\sigma_\ell(\bar{V}_v + \Delta V_v, \bar{V}_\ell)$, $\sigma_\ell(\bar{V}_v, \bar{V}_\ell + \Delta V_\ell)$, and $\sigma_\ell(\bar{V}_v, \bar{V}_\ell)$ are computed according to the deterministic landing analysis procedure outlined earlier.

Gust analysis.- The main drawback of the discrete gust approach is that it depends on a standard gust profile shape which cannot be derived on a logical basis by either theory or experiment and which cannot take into account the random and continuous nature of atmospheric turbulence. Hence, a probabilistic approach which permits description of the random atmospheric turbulence and the associated airplane response in analytic form, should be used. If the atmospheric turbulence is considered a stationary random process, power spectral methods can be used for finding the root-mean-squared values of the stresses induced in the airplane wing structure.

It is well-known (ref. 16) that if $\phi(\tau)$ represents a stationary random disturbance such as the atmospheric vertical velocity and $\psi(\tau)$ denotes a system response, such as the induced stress, then the power spectrum of the response is given by

$$\Phi_\psi(\omega) = |H(\omega)|^2 \Phi_\phi(\omega) \tag{32}$$

where

$\Phi_\phi(\omega)$ spectrum of the disturbance, or input

$\Phi_\psi(\omega)$ spectrum of the response, or output

$|H(\omega)|$ amplitude of the frequency response function, which is defined as the system response to a sinusoidal disturbance of frequency ω

In equation (32), the system is assumed to be linear and the turbulence one-dimensional (i.e., at any instant of time, the vertical gust velocity is constant along the wing span, or the scale of turbulence or the area under the correlation curve (ref. 17) is very large compared with the span of the wing). The spectrum of the response can be used to determine the root-mean-squared value of the response S_ψ as

$$S_\psi^2 = \int_{-\infty}^{\infty} \Phi_\psi(\omega)\, d\omega \tag{33}$$

In the present work, the spectrum of the vertical gust velocity is taken as (Dryden's model (ref. 18))

$$\Phi_\phi(\omega) = \frac{2L}{V_g}\left\{\frac{1 + \left(3L^2\omega^2/V_g^2\right)}{\left[1 + \left(\omega^2 L^2/V_g^2\right)\right]^2}\right\} S_\phi^2 \tag{34}$$

where S_ϕ is the root-mean-squared value of the gust velocity given by

$$S_\phi^2 = \int_{-\infty}^{\infty} \Phi_\phi(\omega)\, d\omega \tag{35}$$

and L is the scale of turbulence and ω is frequency. The integral of equation (33) is evaluated by a numerical procedure involving the evaluation of the spectrum of the response for several values of the frequency. For each frequency ω, the frequency response function $H(\omega)$, and hence the spectrum of the response, is computed by finding the stress response at a point in the airplane wing due to a unit sinusoidal gust. Since this sinusoidal gust can be treated as discrete, the deterministic gust analysis procedure outlined earlier is used to find the transfer function $H(\omega)$. Thus it becomes necessary to use the deterministic gust analysis a number of times in one probabilistic gust analysis.

RESULTS AND DISCUSSION

The design of two example wings is considered for illustrating the optimization procedure. The details of analysis and the numerical results are given below.

Double-Wedge Airfoil (Example 1)

The first example is the design of a hollow symmetric double-wedge airfoil shown in figure 2. The airfoil thickness (t) and chord length (c) are the design variables and the structural mass is the objective function. This design problem is solved by minimizing the energy required to drive the airfoil through a specified flight condition as an alternative objective. The two objective functions are given by

$$f_1(\vec{X}) = \frac{1}{2}\rho_m \ell \rho_s tc \tag{36}$$

and

$$f_2(\vec{X}) = DU\tau_f \tag{37}$$

where ρ_m is the density of the structural material, ℓ is the semispan, ρ_s is the solidity ratio of the wing, D is the total drag, U is the flight velocity, and τ_f is the duration of the flight. The total drag can be expressed as (refs. 1 and 3)

$$D = D_p + D_f \tag{38}$$

where D_p and D_f represent the pressure and the friction drag with

$$D_p = \sum_{i=1}^{N} 2\gamma p_\infty M \left[\alpha_o + \alpha_i + \left(\frac{t}{c}\right)^2\right] \frac{c\ell}{N} \tag{39}$$

$$D_f = \sum_{i=1}^{N} \left[\frac{2\ell}{N} \int_{-c/2}^{c/2} \tau_f'(x) \cos(\alpha_o + \alpha_i) \, dx \right] \tag{40}$$

and

$$\tau_f'(x) = \frac{0.259 p_\infty M^2}{(1 + 0.13M^2)} \left\{ \log_{10} \frac{(1.51 \times 10^5) p_\infty M [T_\infty (1 + 0.13M^2) + 110.39] \left(x + \frac{c}{2}\right)}{T_\infty^2 (1 + 0.13M^2)^{2.5}} \right\}^{-2.584} \tag{41}$$

In equations (39) to (41), p_∞ denotes the atmospheric pressure, γ the ratio of specific heats, M the flight Mach number, N the number of segments of the airfoil, and τ_f' the shear stress.

The design data are given in table I. For the purpose of structural analysis, the semispan of the airfoil is divided into five equal segments, and the bending and torsional flexibility influence coefficients are used to find the steady-state stresses and the natural frequencies of the airfoil by using standard methods of structural analysis (ref. 1). The first bending and the first torsional modes of the airfoil are used as generalized coordinates for the bending-torsion flutter analysis of the structure. The airfoil is assumed to fly at a Mach number of 2.0 during steady-state flight. Piston theory is used for determining the root angle of attack, the static loads producing tip deflection and steady-state stress, the flutter velocity, and the aerodynamic drag of the airfoil.

The optimum solutions are found graphically by plotting the contours of the objective functions (eqs. (36) and (37)) and the constraint boundaries. The contours of the objective functions in the design space are shown in figure 3. For the deterministic approach, the feasible design space and the optimum points are indicated in figure 4. If the structural mass of the airfoil is minimized, the optimum solution corresponds to point D_1 in figure 4 with

$$\vec{X}^* = \begin{Bmatrix} x_1^* \\ x_2^* \end{Bmatrix} \equiv \begin{Bmatrix} t^* \\ c^* \end{Bmatrix} = \begin{Bmatrix} 0.3195 \text{ m} \\ 2.22 \text{ m} \end{Bmatrix}$$

and $f^* = 1077.6$ kg. This solution corresponds to an energy of 162.54 GJ. It can be seen that the upper bounds on the root angle of attack and the landing stress are active at the optimum point. On the other hand, if the energy is minimized, the optimum solution is given by point D_2 with $\vec{X}^* = [0.246 \text{ m}, 3.81 \text{ m}]^T$ and $f^* = 80$ GJ. This solution corresponds to a structural mass of 1422.0 kg. The lower bound on the torsional frequency and the upper bound on the landing stress are active at this optimum point. These results can be used to determine the mass penalty to be paid when minimizing energy or the energy penalty when minimizing structural mass. The point D_1 corresponds to $t/c = 0.144$, while the point D_2 corresponds to $t/c = 0.065$. A smaller value of t/c is required to reduce the energy, while a larger value is required to reduce the structural mass of the wing, as would be expected.

For the probabilistic approach the contours of the objective functions, constraint boundaries, and the feasible design space are shown in figure 5. The optimum solutions corresponding to minimum mass and minimum energy are given by points P_1 and

P_2, respectively. The point P_1 corresponds to $\vec{X}^* = [0.360\ m, 2.220\ m]^T$ with a mass (minimum) of 1217.7 kg and an energy of 196.38 GJ. The point P_2 represents the design vector $\vec{X}^* = [0.276\ m, 4.305\ m]^T$ which corresponds to a mass of 1810.15 kg and an energy (minimum) of 86.2 GJ. It can be seen that the points P_1 and P_2 correspond to t/c equal to 0.162 and 0.064, respectively. As in the deterministic case, a smaller value of t/c is necessary to reduce the energy, while a larger value is necessary to reduce the structural mass of the wing.

For the same value of the permissible landing and/or gust stress, the minimum value of the objective function is higher if probabilistic analysis is used instead of deterministic analysis. For example 1, the optimum points corresponding to minimum mass are D_1 (with $f^* = 1077.6$ kg) for the deterministic analysis and P_1 (with $f^* = 1217.7$ kg) for the probabilistic analysis. Thus the minimum mass from the probabilistic analysis is 140.1 kg higher.

Supersonic Transport Wing (Example 2)

The design of the supersonic wing structure shown in figure 6 is the second example. The overall dimensions of this wing correspond approximately to those of the Concorde wing. The design data are shown in tables II and III. The wing is modeled with three types of finite elements. Constant strain triangular membrane elements represent the wing cover panel, quadrilateral shear web elements represent the ribs and spars, and pin-jointed bar elements represent the axial-load-carrying capacity of ribs and spars. The structural mass is the objective function. Six design variables are used in the optimization, the first four corresponding to the thickness of the skin in the four regions indicated in figure 6(a), the fifth one denoting the thickness of the rib and spar webs, and the sixth one representing the cross-sectional areas of the pin-jointed bars.

A clamped boundary condition is specified along the root of the wing. Only the top half of the wing is idealized for the finite-element analysis by using equivalent plate elements. Since the load vector in the steady-state design condition depends on root angle of attack as well as on displacement state (i.e., nodal displacements), an iterative process was used to determine the correct values of the root angle of attack and the nodal displacements, which provide the specified gross lift (ref. 19). The stress state induced in the finite elements is determined from the known nodal displacements according to the stress-strain and the strain-displacement relations of linear elasticity. The maximum principal stress at the root of the wing σ_s is then computed.

The natural frequencies and mode shapes of the wing are found by setting up the eigenvalue problem and by reducing its order to one-third of that of the corresponding static problem. With Guyan's reduction technique (ref. 20), only the transverse displacement degrees of freedom are retained.

The flutter problem is formulated by using the first four natural vibration modes as generalized coordinates and is solved by using a double iterative scheme (ref. 4). Piston theory (ref. 21) is used for computation of the root angle of attack, the aerodynamic loads producing tip deflection and steady-state stress, and the flutter velocity of the wing structure. The rigid body mode and first bending mode are used as generalized coordinates in the landing and gust stress analysis.

The number of degrees of freedom considered in the finite-element analysis and the number of modes considered in the dynamic analysis are kept low for computational convenience.

A computer program was developed for implementing the present analysis (including the static, eigenvalue, and flutter analysis, and the deterministic or probabilistic landing and gust stress analysis) in conjunction with the optimization program. This program was used for solving the two numerical examples. For example 2, the results obtained using the deterministic approach are shown in tables IV and V. It can be seen that the design variables x_2, x_5, and x_6 attained their lower bounds and x_3 nearly reached its lower bound at the optimum point. Among the behavior constraints, the lower bound constraint on the second natural frequency was active and the flutter speed was near its lower bound. The reduction in structural mass obtained at various stages (iterations) of optimization is shown in figure 7. The reduction in the objective function is negligible after 12 iterations.

In practice, the optimum values of design variables must be rounded off to the nearest practical values. In some cases the designer may be interested in altering the optimum design variables to satisfy certain new design requirements. When the various design variables are changed, the values of the objective function and the response quantities also change. Hence, a sensitivity analysis of the objective function and the behavior constraints with respect to changes in various design variables was conducted at the optimum point. The optimum design was taken as the reference design and the value of each of the design variables was changed by ±30 percent in steps of 10 percent.

Figure 8 shows the results of this sensitivity analysis. The structural mass (fig. 8(a)) is quite sensitive to variation of the design variable x_1. Figures 8(d) and 8(e) show that σ_s and σ_g are also most sensitive to variations of x_1. However, ω_2 (fig. 8(b)) and V_F (fig. 8(c)) are most sensitive to x_4. For example, changing any one of the design variables x_1, x_2, x_3, x_5, or x_6 within ±30 percent of their optimum values does not violate the constraint on V_F; but reducing x_4 by more than 15 percent does violate this constraint. Figure 8 can also be used to identify the less sensitive design variables, so that the designer need not consider them while designing a similar system.

The initial design vector used in the deterministic approach violated the probabilistic landing and gust stress constraints. Hence a different vector is used as the initial (feasible) design vector for the probabilistic optimization approach. All the lower and upper bounds on the response quantities and the design variables were the same. The results of optimization are shown in tables VI and VII. The minimum mass from the probabilistic analysis is 3645.4 kg, while the corresponding value from the deterministic analysis is 2858.4 kg. Thus the optimum value of the objective function is higher in the probabilistic approach.

The design variables x_2, x_3, x_5, and x_6 assumed their lower bounds at the optimum point. Among the behavior constraints, the lower bound on the second natural frequency and the upper bound on the gust stress are active at the optimum point.

Comparing the results obtained using the deterministic and probabilistic approaches leads to the following conclusions:

1. The optimum value of the mass is higher if a probabilistic approach is used for the computation of the landing and gust stresses.

2. The set of active behavior constraints at the optimum point is different for the deterministic and probabilistic approaches.

3. The design variables x_2, x_3, x_5, and x_6 assume their respective lower bounds for both approaches.

These design variables may not reach their lower bounds if the maximum principal stresses used in the constraint equations (7) to (9) are determined by considering all points of the wing structure instead of only those at the root of the wing.

CONCLUDING REMARKS

A procedure is described for the automated optimum design of airplane wing structures with consideration of the stresses developed due to landing and gust loads along with the static strength and flutter constraints. Both deterministic and probabilistic approaches are used for finding the landing and gust stresses. The procedure is demonstrated by considering the design of two example wings: one based on simple beam-type analysis and the other based on finite-element analysis.

The optimization results indicate that for the same value of the permissible landing or gust stress, the minimum value of the objective function is higher if probabilistic analysis is used instead of deterministic analysis. Since the actual values of the stresses induced due to landing and gust loads cannot be predicted precisely, the probabilistic approach is expected to be more accurate and, hence, should be used in the optimum design of airplane wing structures. The procedure outlined is expected to be useful during preliminary design of an airplane structure.

A sensitivity analysis was performed on the optimization results for the finite-element model. The results show that the structural mass, the maximum steady-state stress, and the maximum gust stress were most sensitive to variation of skin thickness near the wing root, while the second natural frequency and flutter speed were most sensitive to variation of skin thickness near the wing tip. These results are expected to be useful when the designer is interested in altering the optimum design variables to satisfy certain new design requirements.

Langley Research Center
National Aeronautics and Space Administration
Hampton, VA 23665
May 19, 1982

REFERENCES

1. Schmit, Lucien A., Jr.; and Thornton, William A.: Synthesis of an Airfoil at Supersonic Mach Number. NASA CR-144, 1965.

2. Stroud, W. Jefferson; Dexter, Cornelia B.; and Stein, Manuel: Automated Preliminary Design of Simplified Wing Structures To Satisfy Strength and Flutter Requirements. NASA TN D-6534, 1971.

3. Miura, Hirokazu: An Optimal Configuration Design of Lifting Surface Type Structures Under Dynamic Constraints. Rep. No. 48, Div. Solid Mech., Struct. & Mech. Design, Case Western Reserve Univ., Oct. 1971.

4. Rao, Singiresu Sambasiva: Automated Optimum Design of Aircraft Wings To Satisfy Strength, Stability, Frequency and Flutter Requirements. Rep. No. 49, Div. Solid Mech., Struct. & Mech. Design, Case Western Reserve Univ., Oct. 1971.

5. Haftka, Raphael T.: Automated Procedure for Design of Wing Structures To Satisfy Strength and Flutter Requirements. NASA TN D-7264, 1973.

6. Sobieszczanski, Jaroslaw; McCullers, L. Arnold; Ricketts, Rodney H.; Santoro, Nick J.; Beskenis, Sharon D.; and Kurtze, William L.: Structural Design Studies of a Supersonic Cruise Arrow Wing Configuration. Proceedings of the SCAR Conference - Part 2, NASA CP-001, [1977], pp. 659-683.

7. Davidson, James W.; Felton, Lewis P.; and Hart, Gary C.: Reliability-Based Optimization for Dynamic Loads. J. Struct. Div., American Soc. Civil Eng., vol. 103, no. ST10, Oct. 1977, pp. 2021-2035.

8. Rao, S. S.: Reliability-Based Optimization Under Random Vibration Environment. Comput. & Struct., vol 14, no. 5-6, 1981, pp. 345-355.

9. Rao, S. S.: Optimization - Theory and Applications. Wiley Eastern, Ltd. (New Delhi), c.1979.

10. Vanderplaats, Garret N.: CONMIN - A Fortran Program for Constrained Function Minimization. User's Manual. NASA TM X-62,282, 1973.

11. Cook, Francis E.; and Milwitzky, Benjamin: Effect of Interaction on Landing-Gear Behavior and Dynamic Loads in a Flexible Airplane Structure. NACA Rep. 1278, 1956. (Supersedes NACA TN 3467.)

12. Houbolt, John C.; and Kordes, Eldon E.: Structural Response to Discrete and Continuous Gusts of an Airplane Having Wing-Bending Flexibility and a Correlation of Calculated and Flight Results. NACA Rep. 1181, 1954. (Supersedes NACA TN 3006; also contains essential material from TN 2763 and TN 2897.)

13. Shufflebarger, C. C.; Payne, Chester B.; and Cahen, George L.: A Correlation of Results of a Flight Investigation With Results of an Analytical Study of Effects of Wing Flexibility on Wing Strains Due to Gusts. NACA Rep. 1365, 1958. (Supersedes NACA TN 4071.)

14. Silsby, Norman S.: Statistical Measurements of Contact Conditions of 478 Transport-Airplane Landings During Routine Daytime Operations. NACA Rep. 1214, 1955. (Supersedes NACA TN 3194.)

15. Ang, Alfredo H-S.; and Tang, Wilson H.: Probability Concepts in Engineering Planning and Design. Volume I - Basic Principles. John Wiley & Sons, Inc., c.1975.

16. Bisplinghoff, Raymond L.; Ashley, Holt; and Halfman, Robert L.: Aeroelasticity. Addison-Wesley Pub. Co., Inc., c.1955.

17. Liepmann, H. W.: On the Application of Statistical Concepts to the Buffeting Problem. J. Aeronaut. Sci., vol. 19, no. 12, Dec. 1952, pp. 793-800, 822.

18. Houbolt, John C.; Steiner, Roy; and Pratt, Kermit G.: Dynamic Response of Airplanes to Atmospheric Turbulence Including Flight Data on Input and Response. NASA TR R-199, 1964.

19. Fox, R. L.; Miura, H.; and Rao, S. S.: Automated Design Optimization of Supersonic Airplane Wing Structures Under Dynamic Constraints. AIAA Paper No. 72-333, Apr. 1972.

20. Guyan, Robert J.: Reduction of Stiffness and Mass Matrices. AIAA J., vol. 3, no. 2, Feb. 1965, p. 380.

21. Ashley, Holt; and Zartarian, Garabed: Piston Theory - A New Aerodynamic Tool for the Aeroelastician. J. Aeronaut. Sci., vol. 23, no. 12, Dec. 1956, pp. 1109-1118.

TABLE I.- DESIGN DATA FOR EXAMPLE 1

Properties of wing:	
Semispan, m	9
Solidity ratio of cross section	0.075
Material (titanium) properties:	
Young's modulus, GPa	110
Shear modulus, GPa	44
Density, kg/m^3	4500
Additional masses:	
Mass of fuel (uniformly distributed in wing), kg	3000
Mass of fuselage, kg	4000
Mass of engine (concentrated 5.4 m from wing root), kg	2000
Static load condition (pull-up maneuver):	
Altitude, m	10 668
Air pressure, Pa	23 844.4
Speed of sound, m/sec	296.7
Air density, kg/m^3	0.3799351
Flight velocity, m/sec	593.4
Duration of flight, sec	5400
Pull-up acceleration	2g
Gust load condition:	
Discrete gust (cosine shape):	
Maximum vertical velocity, m/sec	3
Length, chords	20
Random gust:	
Standard deviation of vertical velocity, m/sec	1
Scale of turbulence, m	762
Forward velocity of flight, m/sec	154.8
Altitude, m	7620
Air density, kg/m^3	0.5494
Landing load condition (fig. 1):	
Unsprung mass below shock strut, kg	320
Landing gear distance from root of wing, m	1.8
Lift factor	1.01
Duration of transient analysis, sec	0.3
Tire force-deflection relation:	
α	1.25×10^6
β	1.22
Inclination of shock strut, rad	0
For deterministic analysis:	
Sink velocity, V_v, m/sec	3
Horizontal velocity at contact, V_ℓ, m/sec	45
For probabilistic analysis:	
$\bar{V}_v$, m/sec	2.3
S_{V_v}	$0.1\bar{V}_v$
$\bar{V}_\ell$, m/sec	34.6
S_{V_ℓ}	$0.1\bar{V}_\ell$

TABLE I.- Concluded

Bounds on design variables and other constraints:

	Lower bound	Upper bound
$x_1 \equiv t$, m	0.18	0.45
$x_2 \equiv c$, m	1.5	4.5
$\omega_1 \equiv \omega_b$, Hz	2.0	4.0
$\omega_2 \equiv \omega_t$, Hz	10.0	30.0
δ, m		1.2
α_o, rad		0.08
V_F, m/sec	890.0	
σ_g, MPa		100
σ_ℓ, MPa		200
σ_s, MPa		800

TABLE II.- DESIGN DATA FOR EXAMPLE 2

Material (aluminum alloy) properties of wing:	
Young's modulus, GPa	68.948
Poisson's ratio	0.3
Density, kg/m^3	2768
Additional masses:	
Maximum take-off mass, kg	174 632.9
Mass of all engines, kg	5669.9
Fuselage and payload, kg	32 658.6
Fuel, kg	41 957.99
Static load condition (pull-up maneuver):	
Altitude, m	7620
Air pressure, Pa	37 649.7
Speed of sound, m/sec	309.7
Air density, kg/m^3	0.5498382
Flight velocity, m/sec	526.49
Pull-up acceleration	3.75g
Gust load condition:	
Discrete gust (cosine shape):	
Maximum vertical velocity, m/sec	1.5240
Length, chords	10
Random gust:	
Standard deviation of vertical velocity, m/sec	0.5080
Scale of turbulence, m	762
Forward velocity of flight, m/sec	154.8
Altitude, m	7620
Air density, kg/m^3	0.5498382
Landing load condition:	
Unsprung mass below shock strut, kg	2264.4
Landing gear location:	
x_ℓ, m	19.3548
y_ℓ, m	2.7737
Lift factor	1.01
Duration of transient analysis, sec	0.6
Tire force-deflection relation:	
α	16.8998
β	1.21
Inclination of strut, rad	0
For deterministic analysis:	
Sink velocity, V_v, m/sec	1.1430
Horizontal velocity at contact, V_ℓ, m/sec	45
For probabilistic analysis:	
$\bar{V}_v$, m/sec	0.8792
S_{V_v}	$0.1\bar{V}_v$
$\bar{V}_\ell$, m/sec	34.6
S_{V_ℓ}	$0.1\bar{V}_\ell$
Number of natural frequencies constrained	2

TABLE III.- THICKNESS AND FUEL DISTRIBUTION

FOR EXAMPLE 2

Planform node number[a]	z-coordinate of top node, mm	Mass of fuel, kg
1	45.72	1961.82
2	35.56	1519.56
3	60.96	1698.73
4	96.01	2694.38
5	55.88	1555.85
6	83.36	2036.66
7	146.30	3447.36
8	111.25	2599.13
9	76.20	1791.72
10	121.92	1258.74
11	177.80	1834.81
12	205.74	2122.85
13	151.13	1555.85
14	96.52	984.31
15	167.64	1950.48
16	231.14	2698.92
17	299.01	3946.32
18	243.84	2855.41
19	180.34	2088.83
20	116.84	1356.26
21	223.52	0
22	297.18	0
23	373.38	0
24	411.48	0
25	320.04	0
26	228.60	0
27	137.16	0

[a]Node numbers are defined in figure 6(b).

TABLE IV.- DETERMINISTIC OPTIMIZATION RESULTS FOR EXAMPLE 2

	Initial design	Bounds		Optimum design
		Lower	Upper	
Design variables:				
x_1, mm	3.81	1.016	12.7	2.7211
x_2, mm	3.81	1.016	12.7	[a]1.0160
x_3, mm	3.81	1.016	12.7	1.0244
x_4, mm	3.81	1.016	12.7	1.4917
x_5, mm	6.35	1.016	12.7	[a]1.0160
x_6, mm^2	161.3	25.8	322.6	[a]25.8
Structural mass of wing (objective function), kg	7323.3			2858.4
Total number of function evaluations required				116
Computer time required,[b] CPU sec				3060

[a]Lower bound value.
[b]Control Data CYBER 175 Computer.

TABLE V.- BEHAVIOR CONSTRAINTS FOR EXAMPLE 2 FROM DETERMINISTIC ANALYSIS

Behavior constraint	Initial design	Bounds		Optimum design
		Lower	Upper	
Wing tip deflection, δ, m	1.0158		1.2700	1.2147
Root angle of attack, α_o, rad (deg)	0.1539 (8.8178)		0.2088 (11.9633)	0.1601 (9.1730)
First natural frequency, ω_1, Hz	0.9615	0.4775	1.5915	0.5777
Second natural frequency, ω_2, Hz	2.6666	1.5915	3.9789	[a]1.5976
Flutter speed, V_F, m/sec	1944.7759	526.5024		601.7922
Steady state stress, σ_s, MPa	275.4886		344.740	[a]338.1141
Landing stress, σ_ℓ, MPa	[a]413.1502		413.688	[a]409.1581
Gust stress, σ_g, MPa	149.6999		206.844	[a]206.8440

[a]Active constraint.

TABLE VI.- PROBABILISTIC OPTIMIZATION RESULTS FOR EXAMPLE 2

	Initial design	Bounds		Optimum design
		Lower	Upper	
Design variables:				
x_1, mm	5.08	1.016	12.7	4.1783
x_2, mm	3.81	1.016	12.7	[a]1.016
x_3, mm	3.81	1.016	12.7	[a]1.016
x_4, mm	3.81	1.016	12.7	1.5519
x_5, mm	6.35	1.016	12.7	[a]1.016
x_6, mm^2	161.3	25.8	322.6	[a]25.8
Structural mass of wing (objective function), kg	7994.5			3645.4
Total number of function evaluations required				82
Computer time required,[b] CPU sec				1648

[a]Lower bound value.
[b]Control Data CYBER 175 Computer.

TABLE VII.- VALUES OF BEHAVIOR CONSTRAINTS FOR EXAMPLE 2

FROM PROBABILISTIC ANALYSIS

Behavior constraint	Initial design	Bounds		Optimum design
		Lower	Upper	
Wing tip deflection, δ, m	0.9806		1.2700	1.2236
Root angle of attack, α_o, rad (deg)	0.1537 (8.8063)		0.2088 (11.9633)	0.1593 (9.1272)
First natural frequency, ω_1, Hz	0.9888	0.4775	1.5915	0.5917
Second natural frequency, ω_2, Hz	2.7158	1.5915	3.9789	[a]1.6325
Flutter speed, V_F, m/sec	1949.0350	526.5024		615.6526
Steady-state stress, σ_s, MPa	224.6464		344.740	238.5946
Landing stress, σ_ℓ, MPa	407.9998		413.688	398.2367
Gust stress, σ_g, MPa	159.8697		206.844	[a]206.4717

[a]Active constraint.

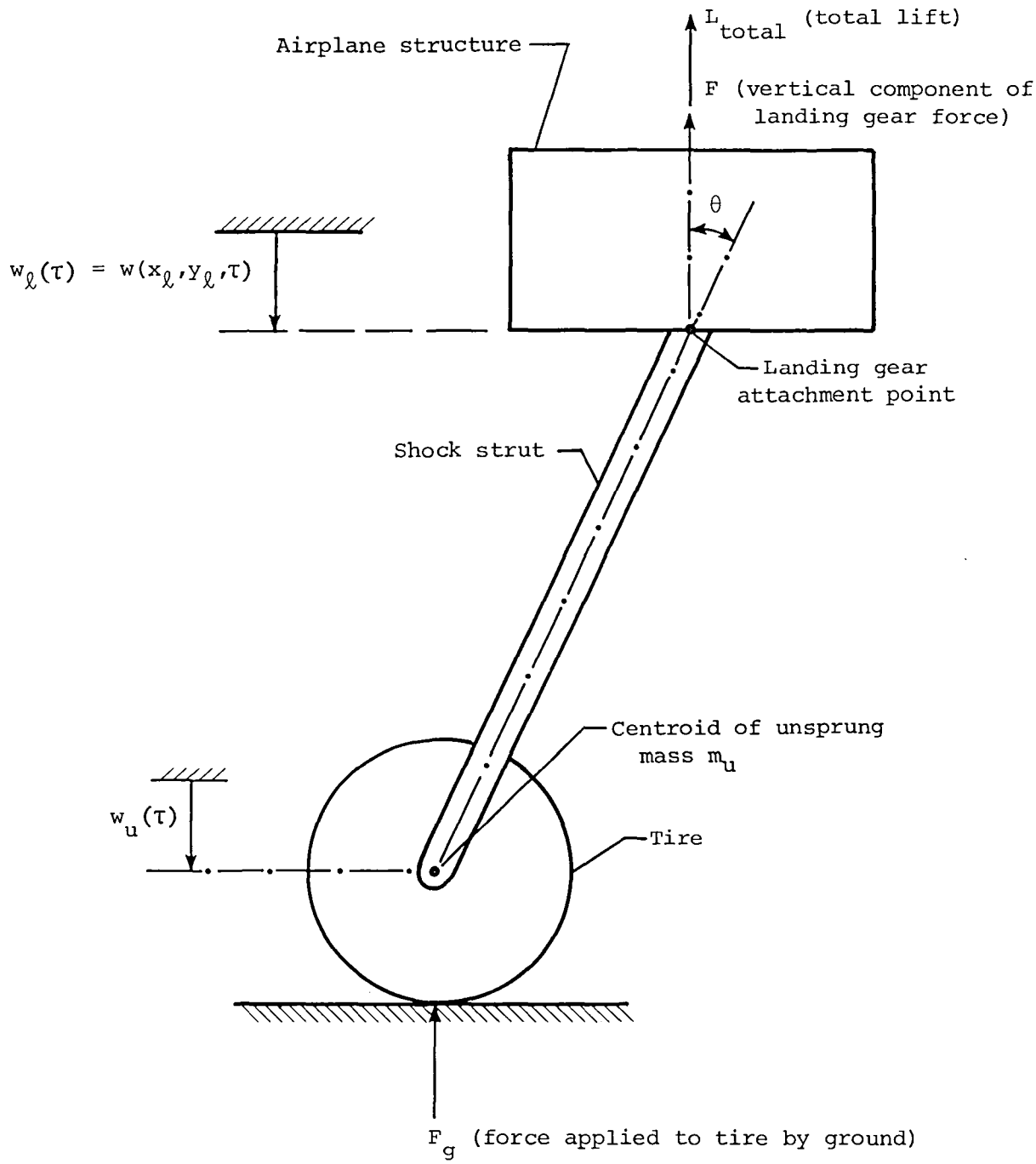

Figure 1.- Landing gear arrangement.

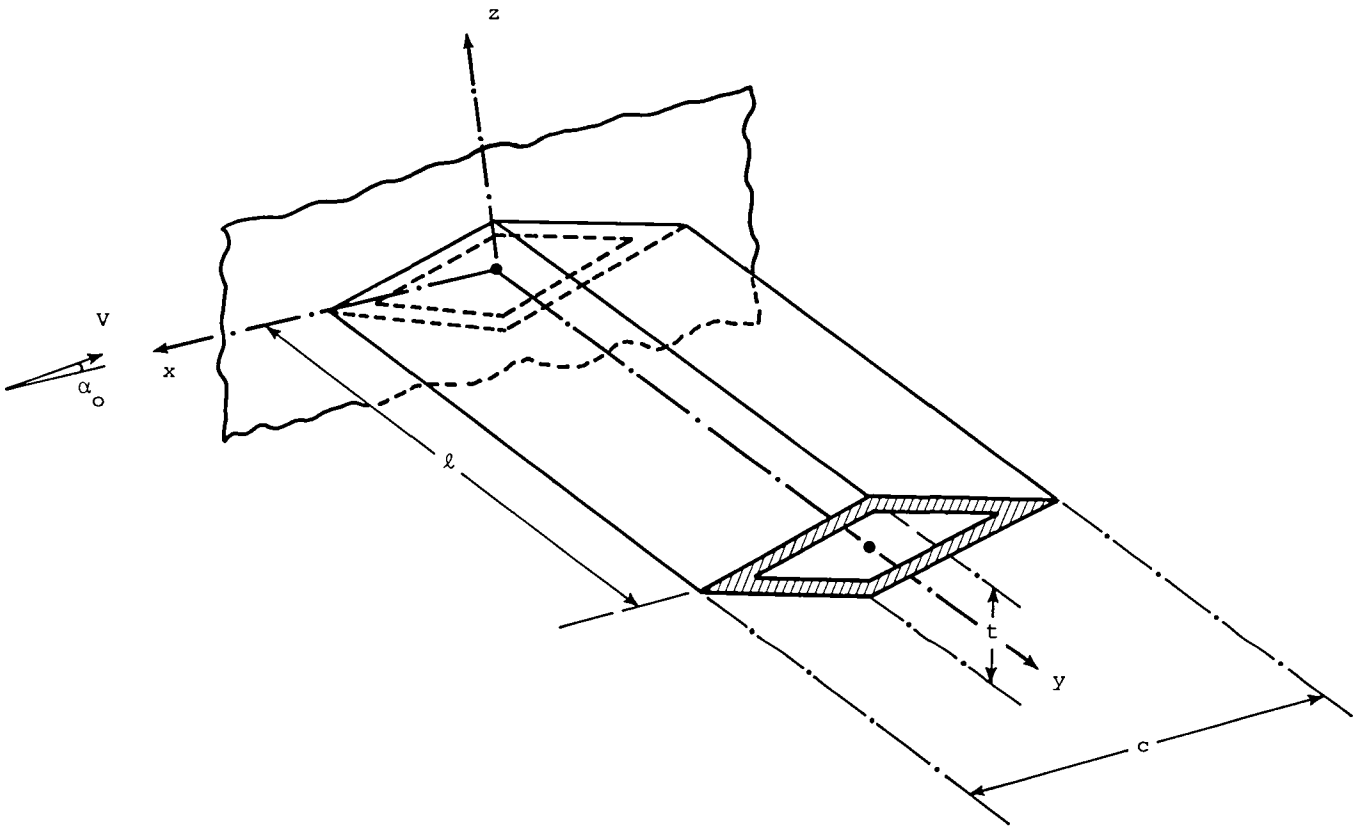

Figure 2.- Double-wedge airfoil (example 1).

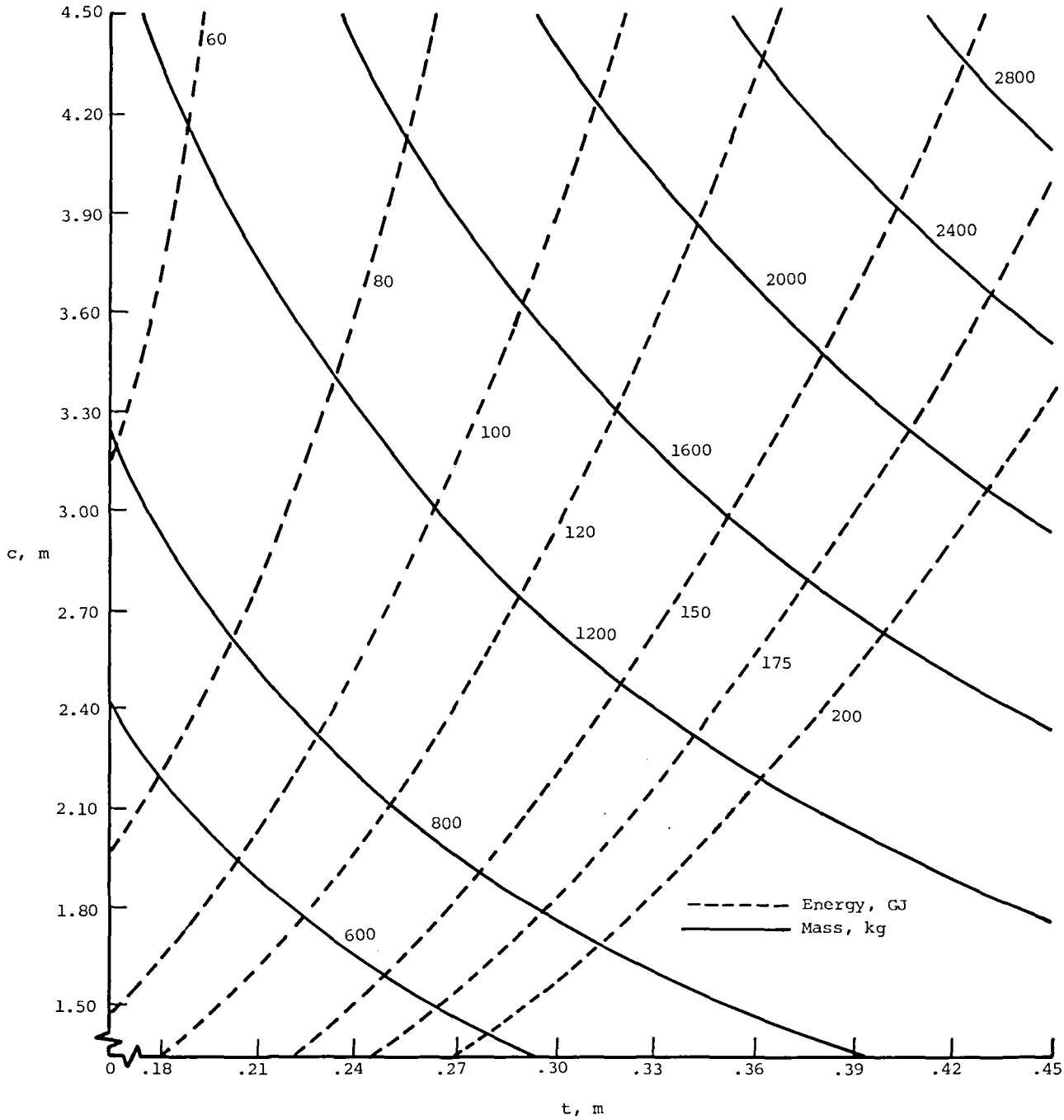

Figure 3.- Contours of objective functions, structural mass, and energy for example 1.

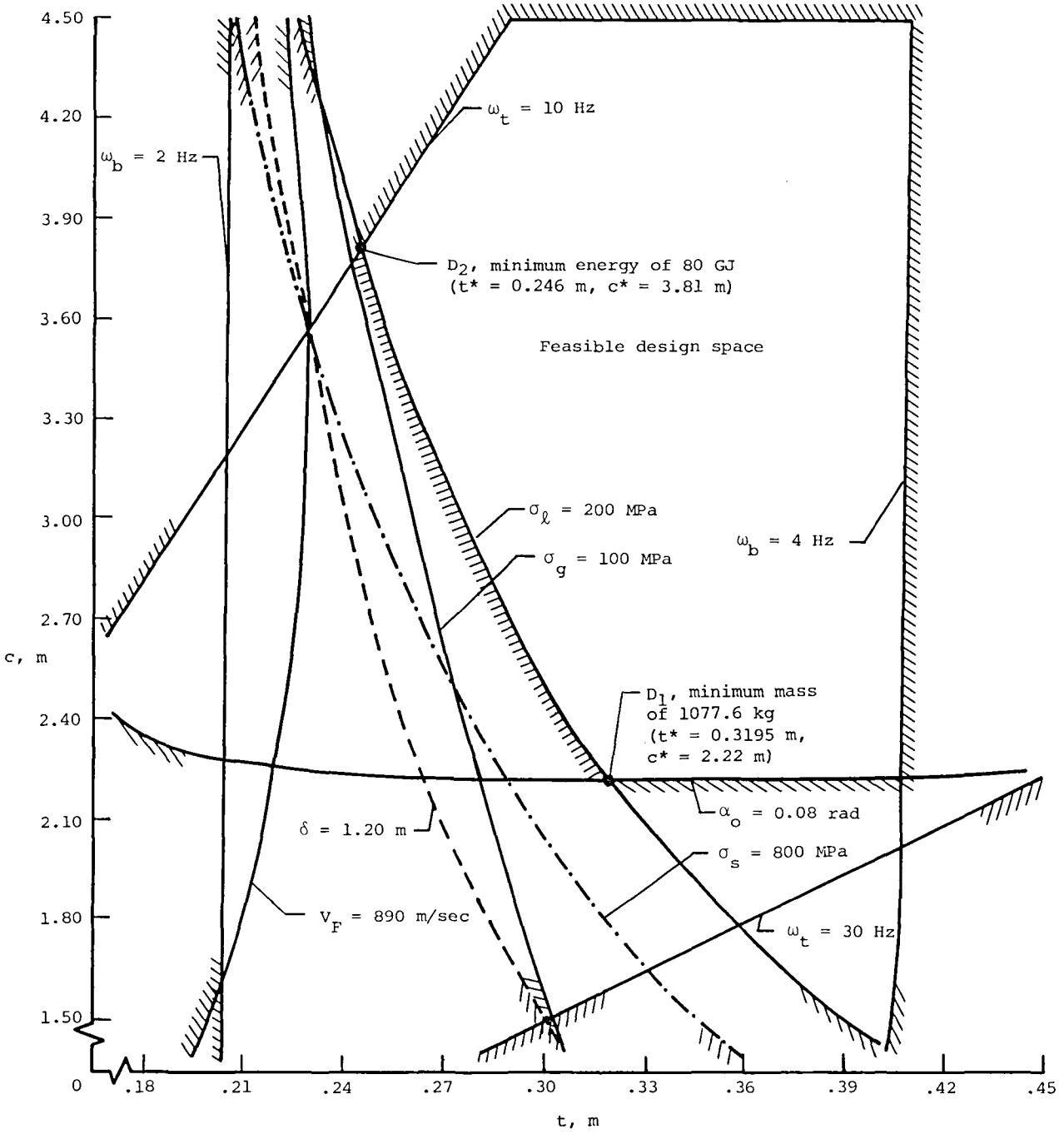

Figure 4.- Graphical optimization of example 1 with deterministic analysis used for σ_ℓ and σ_g.

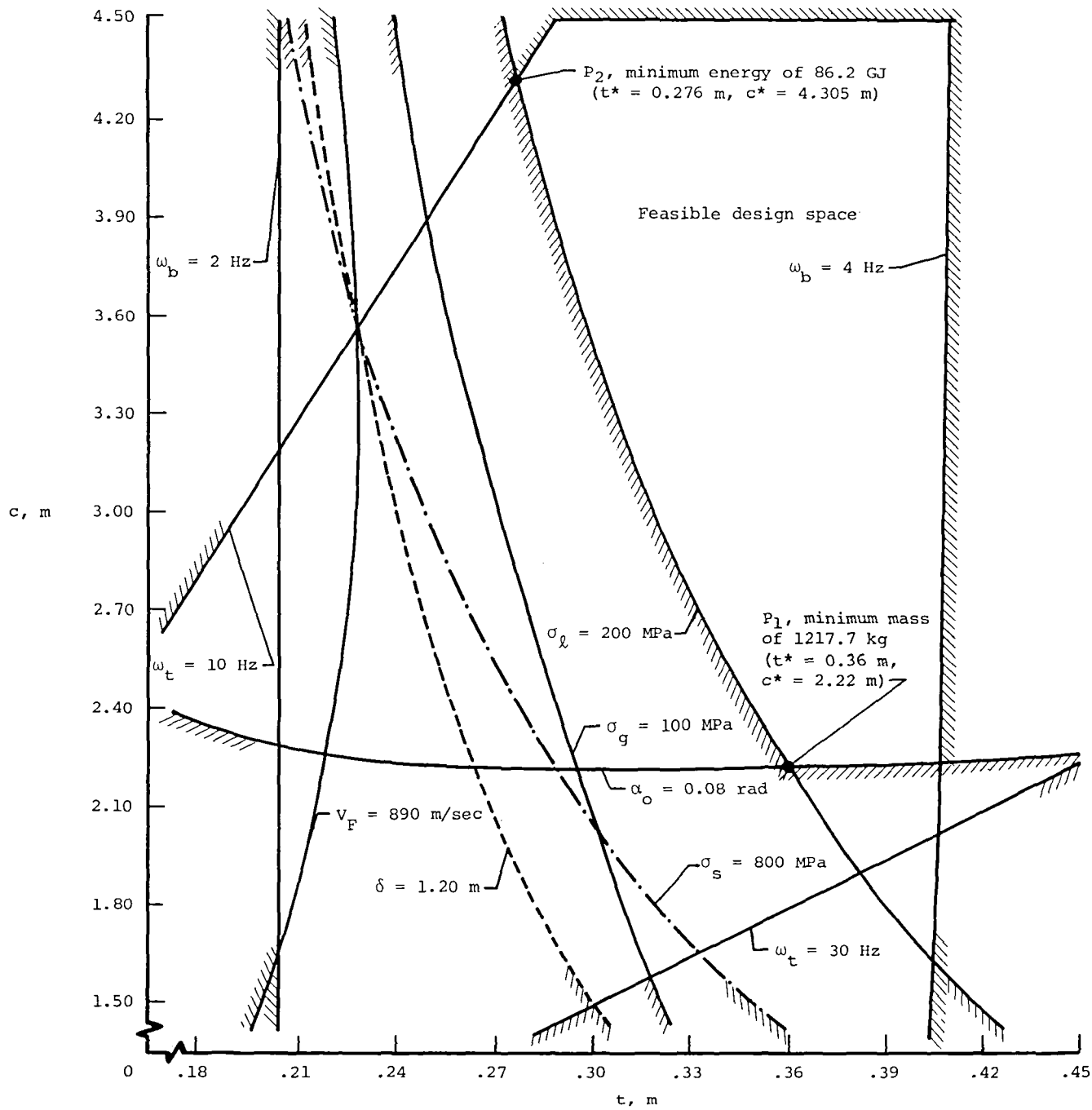

Figure 5.- Graphical optimization of example 1 with probabilistic analysis used for σ_ℓ and σ_g.

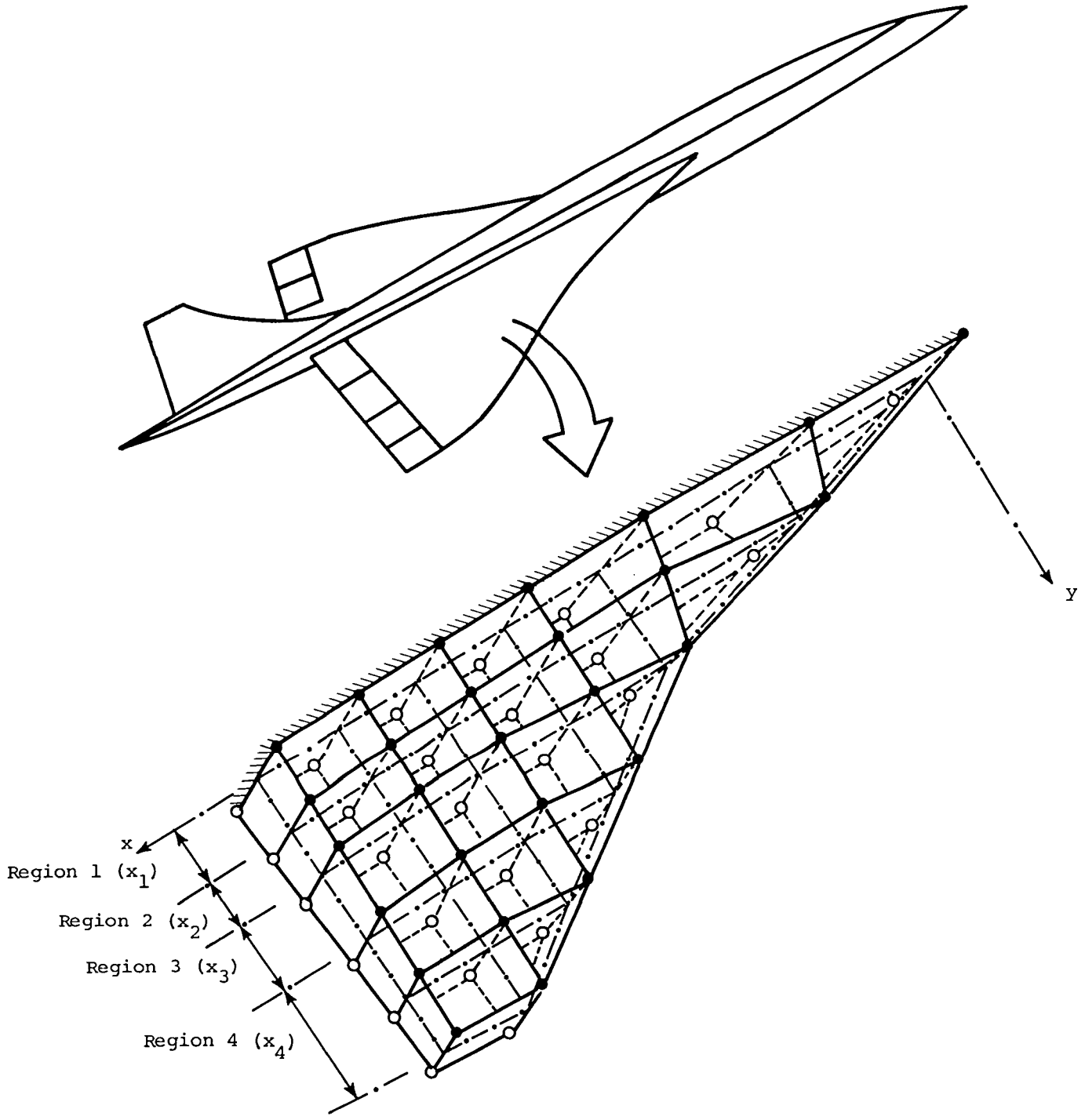

(a) Finite-element idealization.

Figure 6.- Supersonic transport wing (example 2).

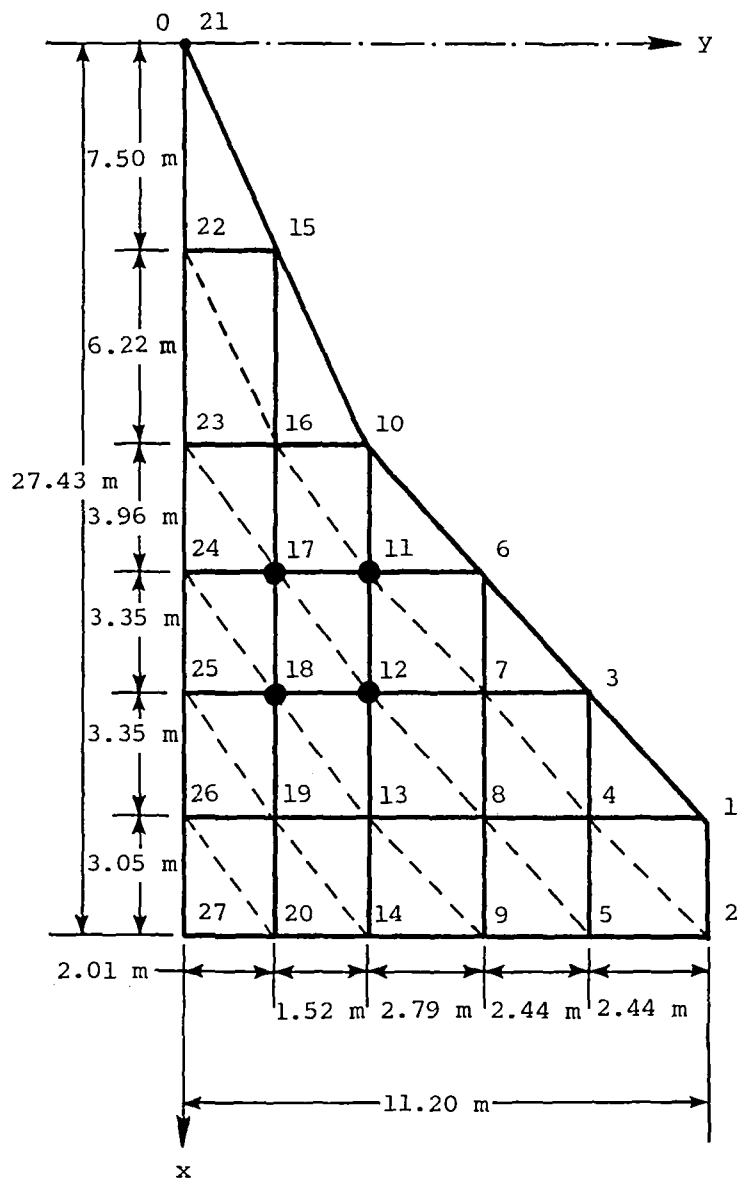

● Engine mass of 1417.5 kg at each of four locations
Solid lines indicate spars and ribs
Dotted lines indicate cover plate finite elements

(b) Planform nodes and geometry.

Figure 6.- Concluded.

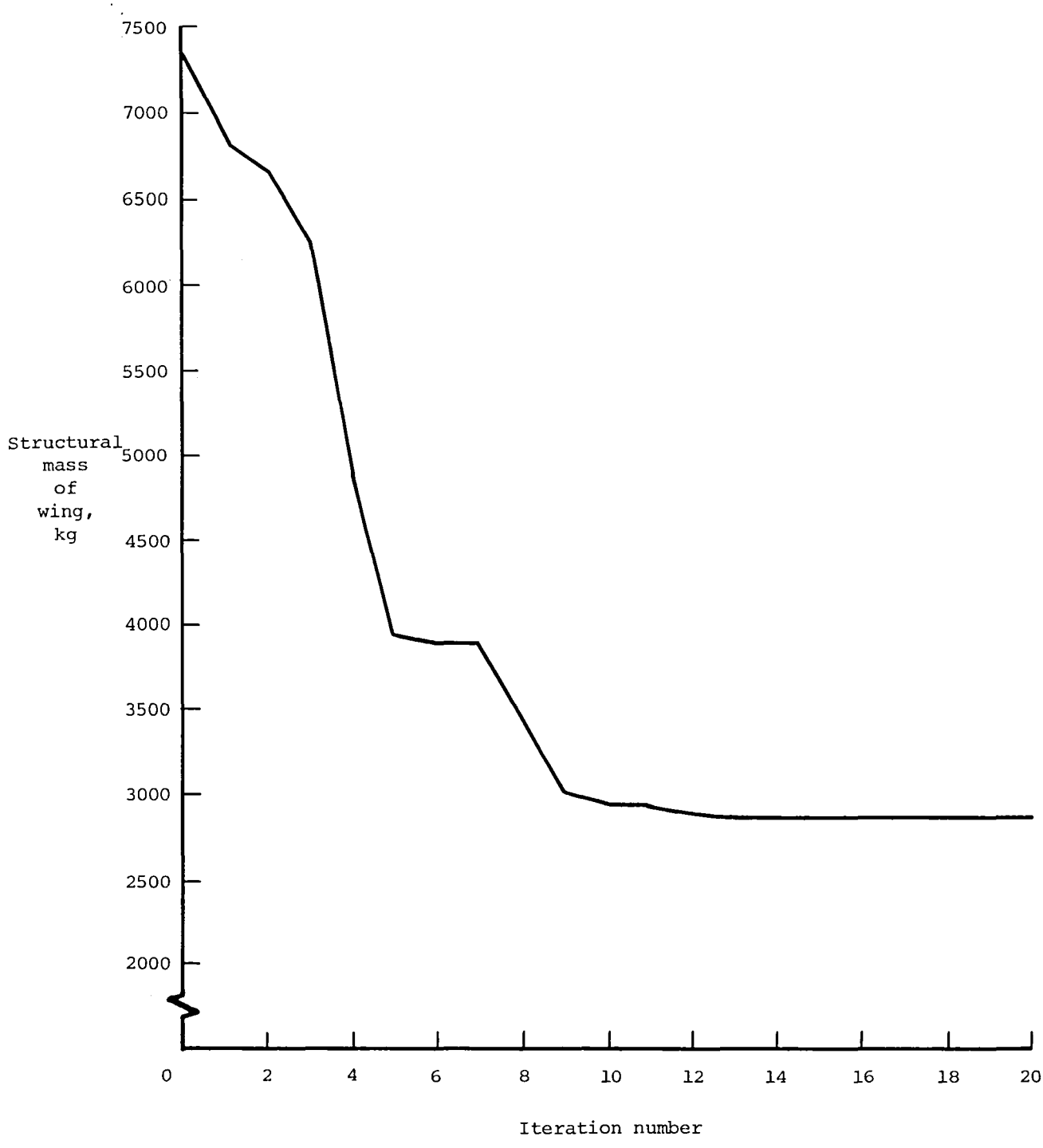

Figure 7.- Convergence of objective function for example 2 with deterministic analysis.

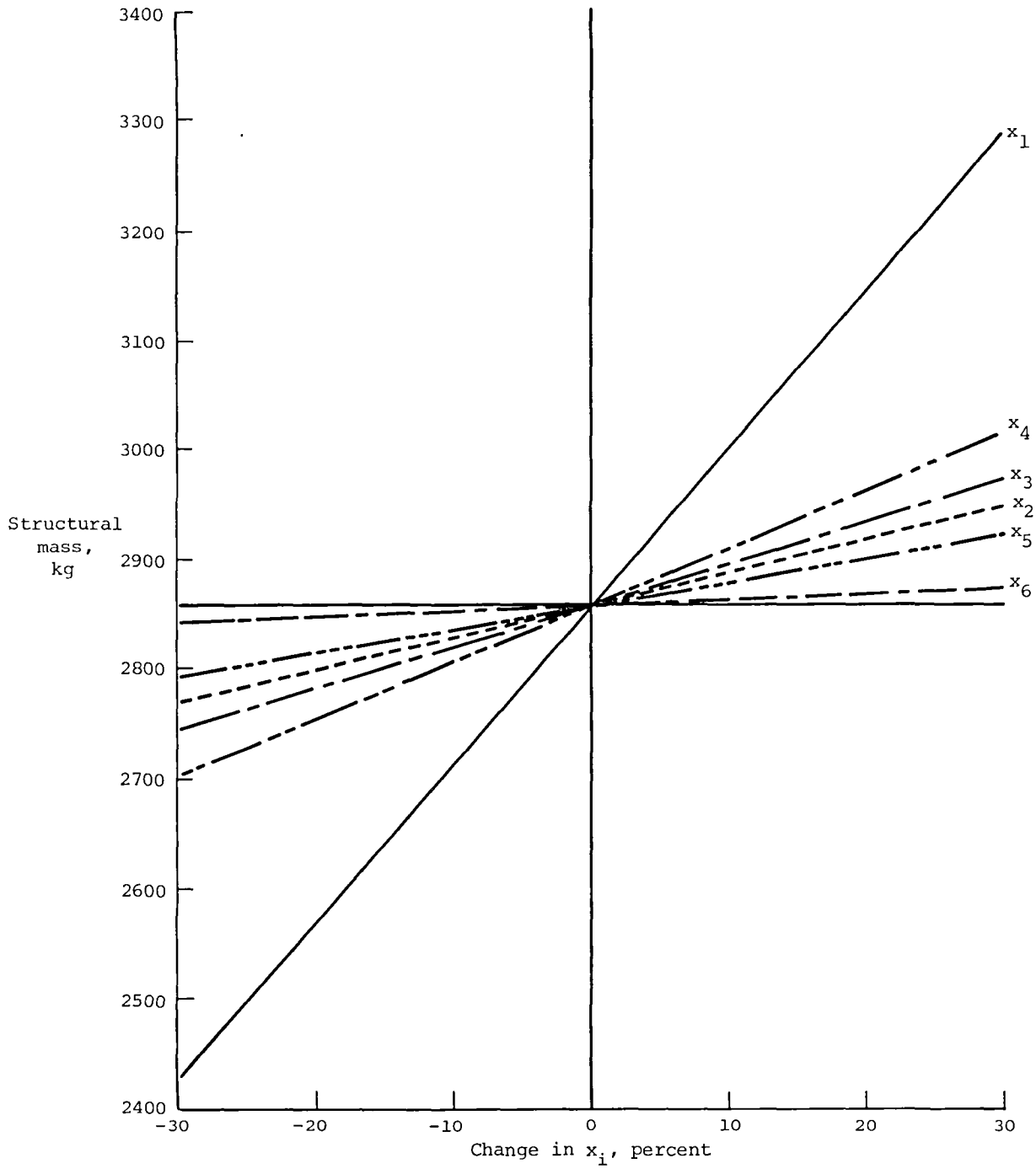

(a) Structural mass.

Figure 8.- Sensitivity of various parameters to design variables for example 2 with deterministic analysis used for σ_ℓ and σ_g.

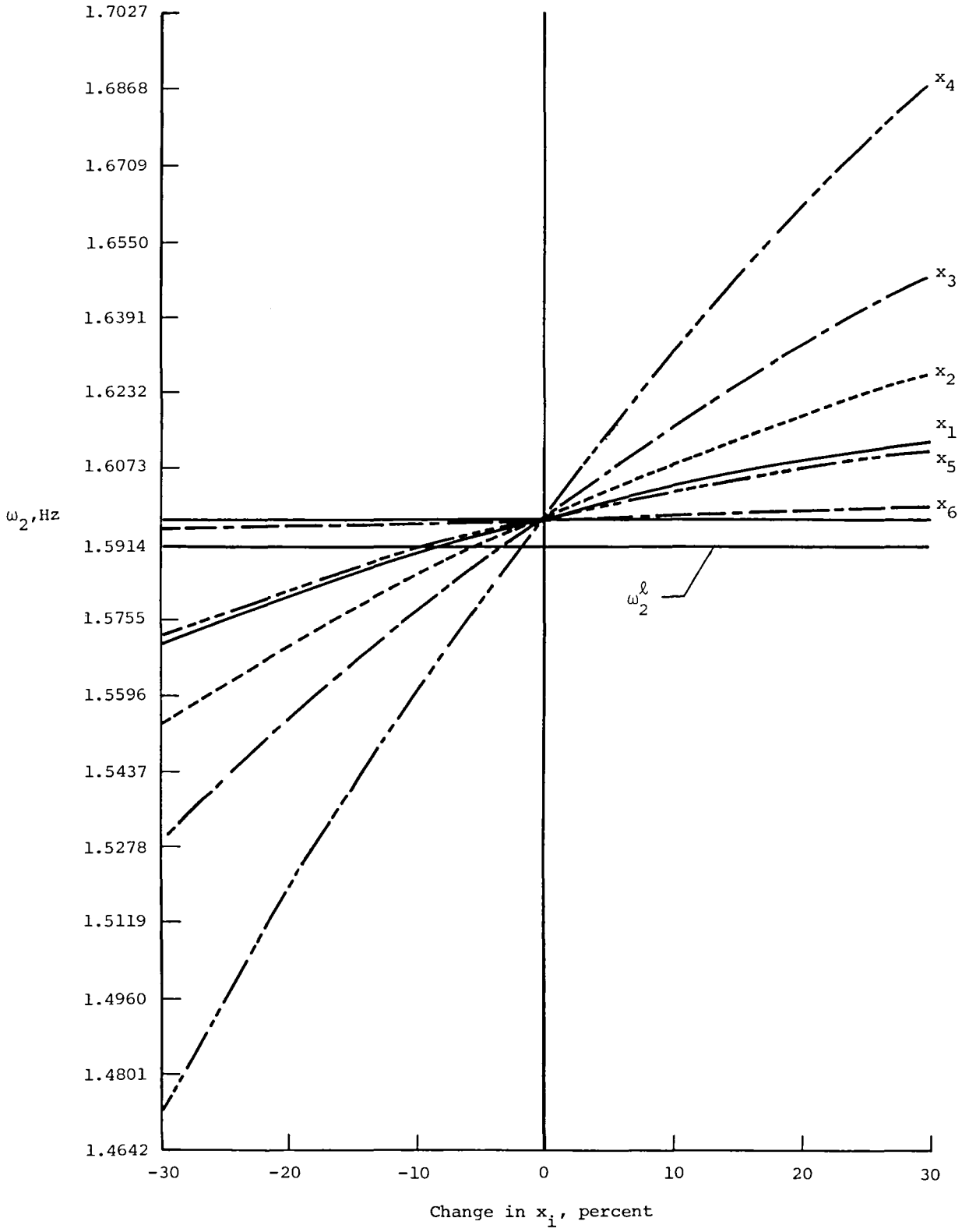

(b) Second natural frequency ω_2.

Figure 8.- Continued.

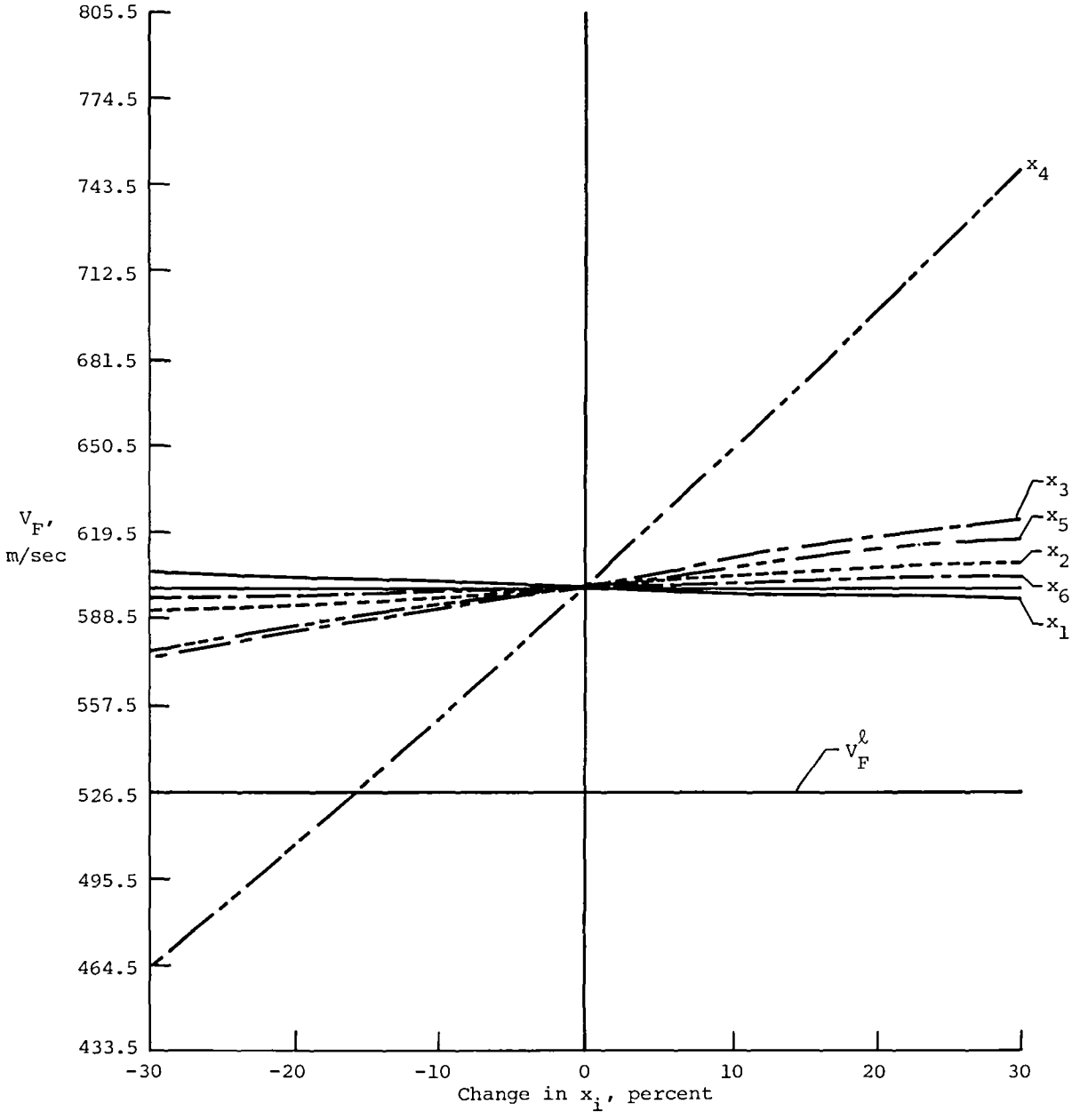

(c) Flutter velocity V_F.

Figure 8.- Continued.

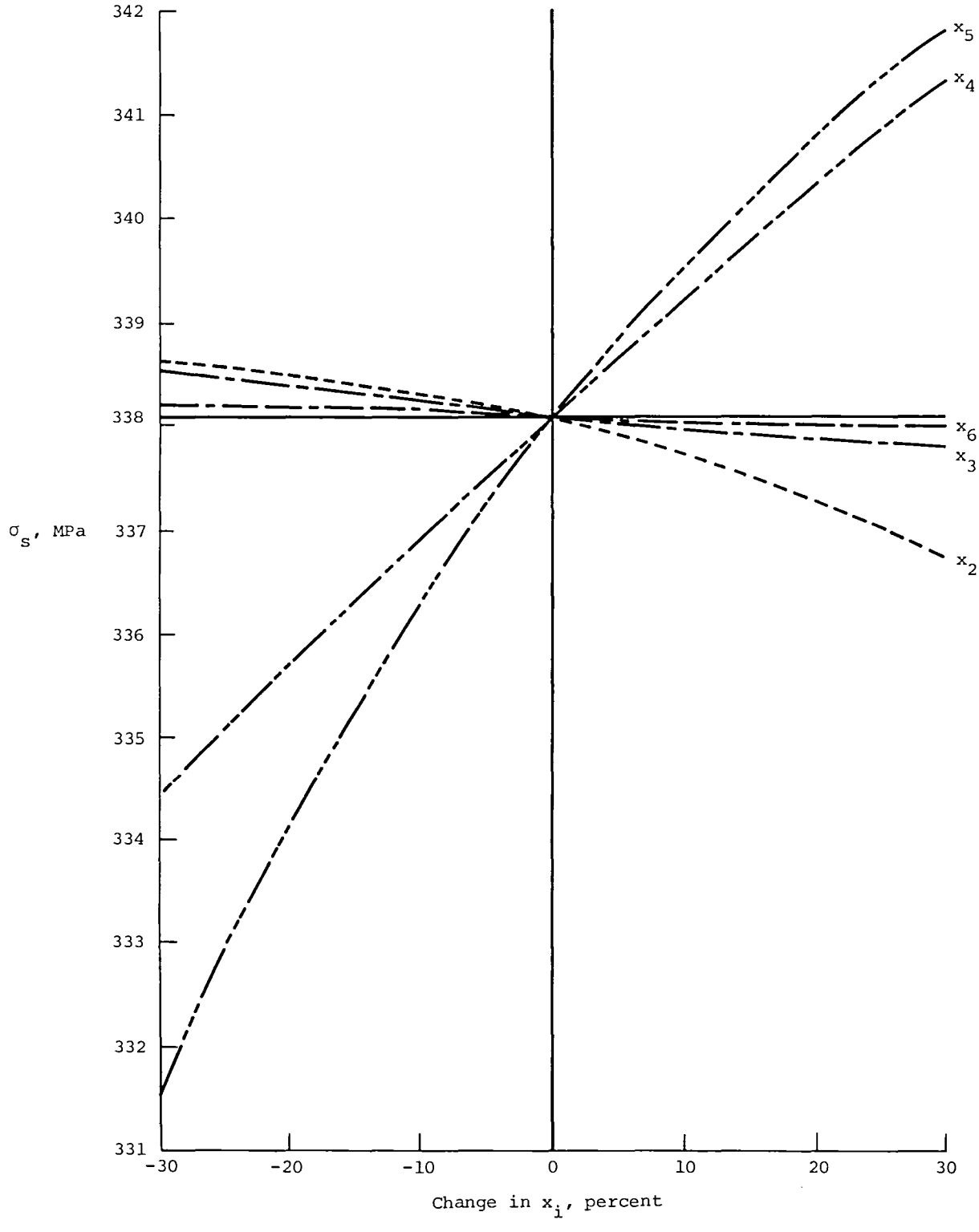

(d) Maximum steady-state stress σ_s.

Figure 8.- Continued.

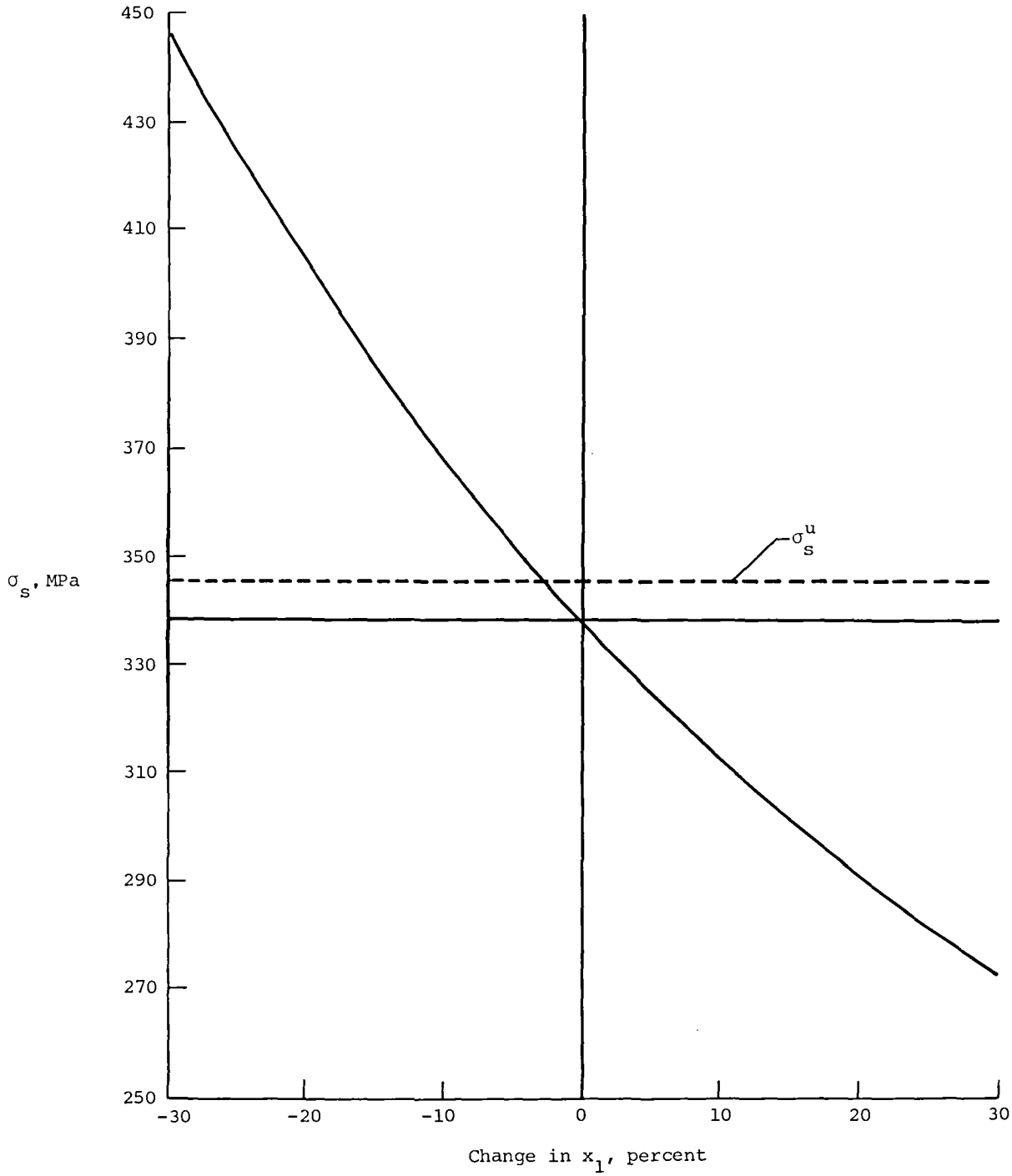

(d) Concluded.

Figure 8.- Continued.

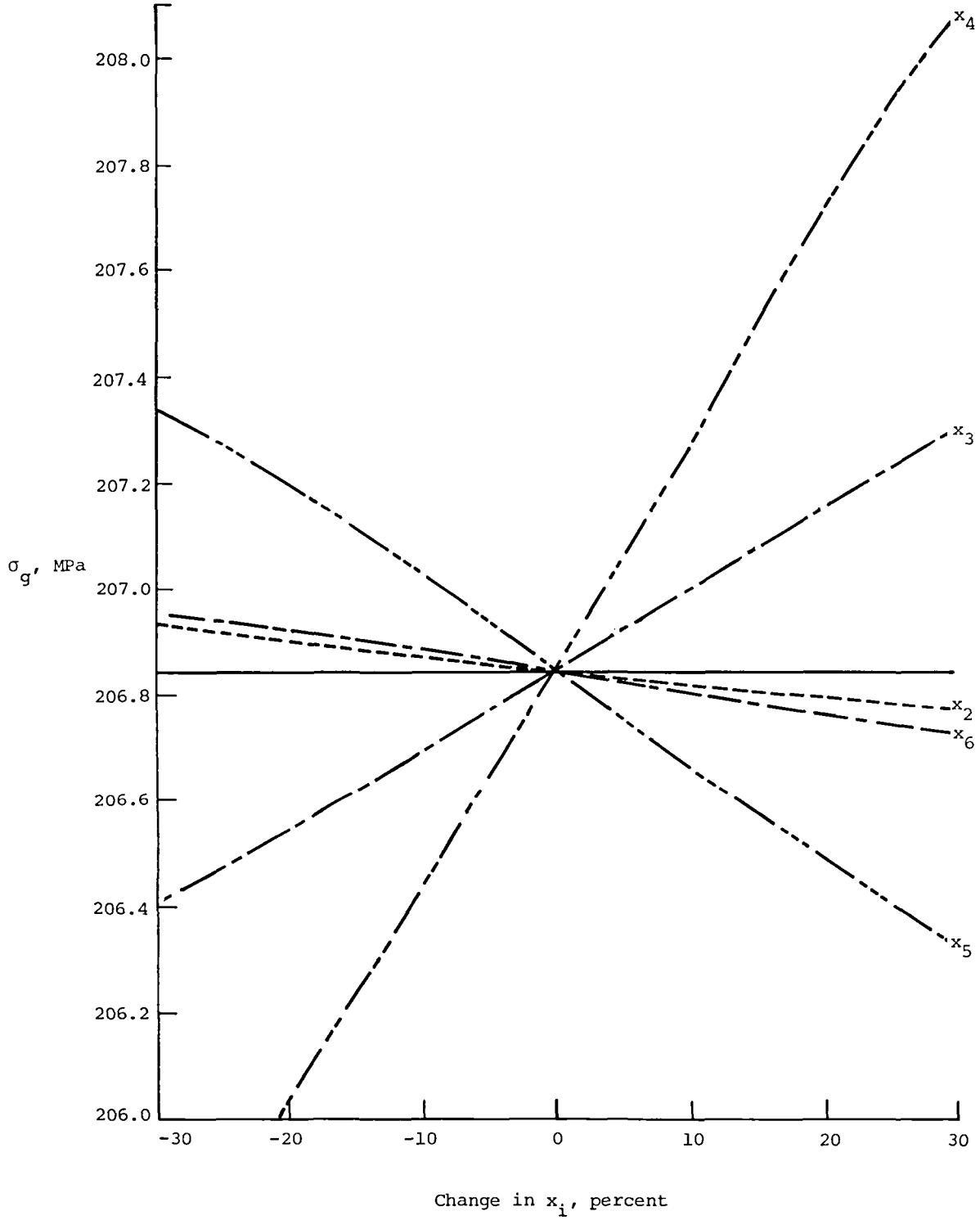

(e) Maximum gust stress σ_g.

Figure 8.- Continued.

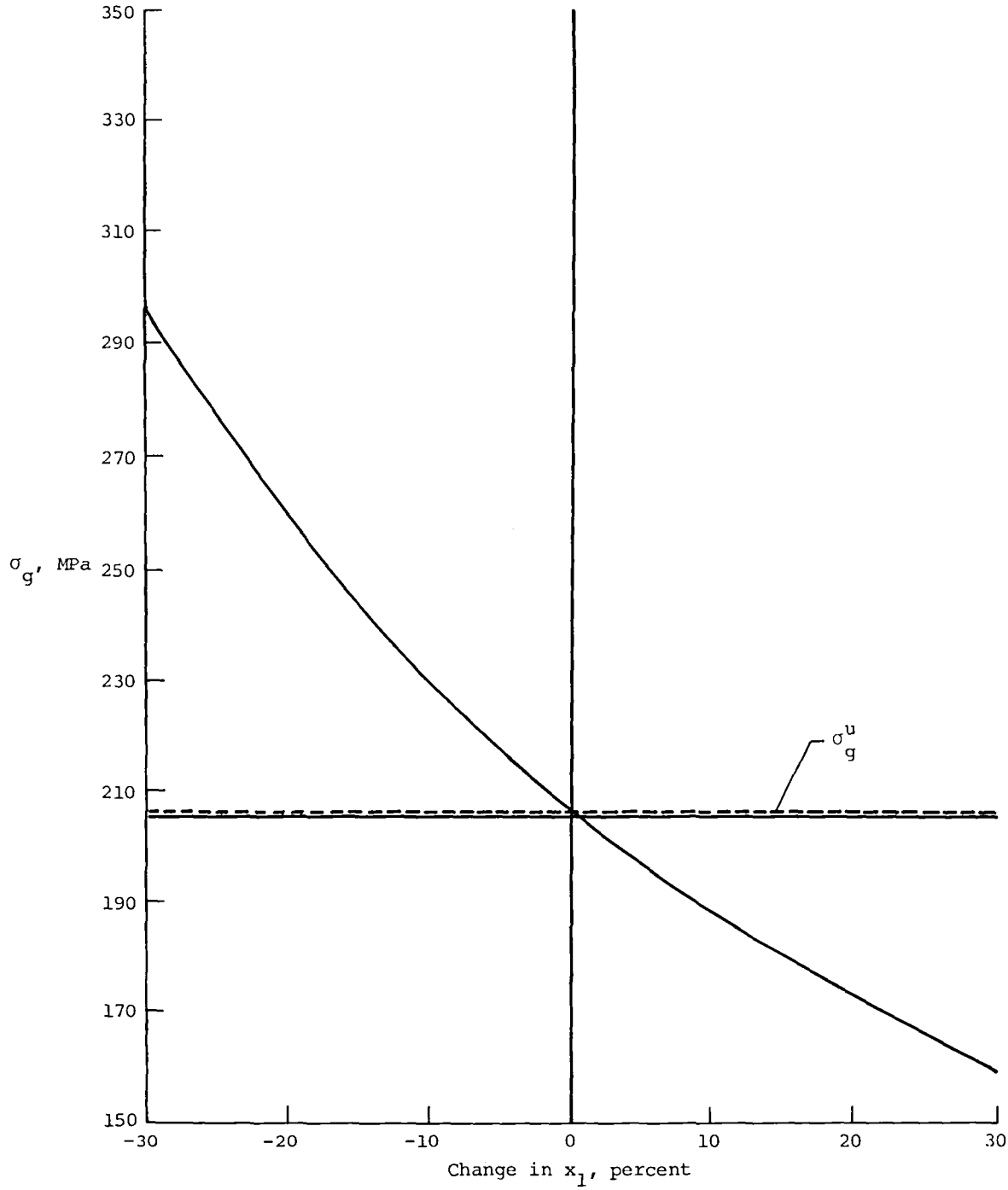

(e) Concluded.

Figure 8.- Concluded.

1. Report No.	2. Government Accession No.	3. Recipient's Catalog No.
NASA TM-84475		

4. Title and Subtitle	5. Report Date
AUTOMATED OPTIMUM DESIGN OF WING STRUCTURES - DETERMINISTIC AND PROBABILISTIC APPROACHES	August 1982
	6. Performing Organization Code 505-33-63-02

7. Author(s)	8. Performing Organization Report No.
S. S. Rao	L-15169
	10. Work Unit No.

9. Performing Organization Name and Address	11. Contract or Grant No.
NASA Langley Research Center Hampton, VA 23665	

12. Sponsoring Agency Name and Address	13. Type of Report and Period Covered
National Aeronautics and Space Administration Washington, DC 20546	Technical Memorandum
	14. Sponsoring Agency Code

15. Supplementary Notes

S. S. Rao: NRC-NASA Senior Research Associate, now at San Diego State University.

16. Abstract

A procedure is described for the automated optimum design of airplane wing structures subjected to multiple behavior constraints. The structural mass of the wing is considered the objective function. Both deterministic and probabilistic approaches are used for finding the stresses induced in the airplane wing structure due to landing and gust loads. The thicknesses of the skin and the web and the cross-sectional areas of the flanges are the design variables, and nonlinear programming techniques are used to find the optimum solution. For the examples considered, the optimum value of the objective function is higher when the landing and gust stresses are treated as random variables than when they are considered deterministic quantities.

17. Key Words (Suggested by Author(s))	18. Distribution Statement
Aircraft design Structural mechanics Optimization	Unclassified - Unlimited Subject Category 05

19. Security Classif. (of this report)	20. Security Classif. (of this page)	21. No. of Pages	22. Price
Unclassified	Unclassified	46	A03

For sale by the National Technical Information Service, Springfield, Virginia 22161

NASA-Langley, 1982

National Aeronautics and
Space Administration

Washington, D.C.
20546

Official Business
Penalty for Private Use, $300

THIRD-CLASS BULK RATE

Postage and Fees Paid
National Aeronautics and
Space Administration
NASA-451

POSTMASTER: If Undeliverable (Section 158 Postal Manual) Do Not Return